


# Oncolytic Orf virus licenses NK cells via cDC1 to activate innate and adaptive antitumor mechanisms and extends survival in a murine model of late-stage ovarian cancer

Jacob P van Vloten,<sup>1</sup> Kathy Matuszewska,<sup>2</sup> Mark A A Minow,<sup>3</sup> Jessica A Minott,<sup>1</sup> Lisa A Santry,<sup>1</sup> Madison Pereira,<sup>2</sup> Ashley A Stegelmeier,<sup>1</sup> Thomas M McAusland,<sup>1</sup> Elaine M Klafuric,<sup>1</sup> Khalil Karimi,<sup>1</sup> Joseph Colasanti,<sup>4</sup> D Grant McFadden,<sup>5</sup> James J Petrik,<sup>2</sup> Byram W Bridle,<sup>1</sup> Sarah K Wootton <sup>1</sup>

**To cite:** van Vloten JP, Matuszewska K, Minow MAA, *et al.* Oncolytic Orf virus licenses NK cells via cDC1 to activate innate and adaptive antitumor mechanisms and extends survival in a murine model of late-stage ovarian cancer. *Journal for ImmunoTherapy of Cancer* 2022;**10**:e004335. doi:10.1136/jitc-2021-004335

► Additional supplemental material is published online only. To view, please visit the journal online (<http://dx.doi.org/10.1136/jitc-2021-004335>).

AAS, TMM and EMK contributed equally.

BWB and SKW are joint senior authors.

Accepted 12 February 2022



© Author(s) (or their employer(s)) 2022. Re-use permitted under CC BY-NC. No commercial re-use. See rights and permissions. Published by BMJ.

For numbered affiliations see end of article.

## Correspondence to

Dr Sarah K Wootton;  
kwootton@uoguelph.ca

## ABSTRACT

**Background** Novel therapies are needed to improve outcomes for women diagnosed with ovarian cancer. Oncolytic viruses are multifunctional immunotherapeutic biologics that preferentially infect cancer cells and stimulate inflammation with the potential to generate antitumor immunity. Herein we describe *Parapoxvirus ovis* (Orf virus (OrfV)), an oncolytic poxvirus, as a viral immunotherapy for ovarian cancer.

**Methods** The immunotherapeutic potential of OrfV was tested in the ID8 orthotopic mouse model of end-stage epithelial ovarian carcinoma. Immune cell profiling, impact on secondary lesion development and survival were evaluated in OrfV-treated mice as well as in Batf3 knockout, mice depleted of specific immune cell subsets and in mice where the primary tumor was removed. Finally, we interrogated gene expression datasets from primary human ovarian tumors from the International Cancer Genome Consortium database to determine whether the interplay we observed between natural killer (NK) cells, classical type 1 dendritic cells (cDC1s) and T cells exists and influences outcomes in human ovarian cancer.

**Results** OrfV was an effective monotherapy in a murine model of advanced-stage epithelial ovarian cancer. OrfV intervention relied on NK cells, which when depleted abrogated antitumor CD8<sup>+</sup> T-cell responses. OrfV therapy was shown to require cDC1s in experiments with BATF3 knockout mice, which do not have mature cDC1s. Furthermore, cDC1s governed antitumor NK and T-cell responses to mediate antitumor efficacy following OrfV. Primary tumor removal, a common treatment option in human patients, was effectively combined with OrfV for optimal therapeutic outcome. Analysis of human RNA sequencing datasets revealed that cDC1s correlate with NK cells in human ovarian cancer and that intratumoral NK cells correlate positively with survival.

**Conclusions** The data herein support the translational potential of OrfV as an NK stimulating immunotherapeutic for the treatment of advanced-stage ovarian cancer.

## Key messages

### What is already known on this topic

► Immunotherapies are under intense investigation for the treatment of ovarian cancer, which is difficult to detect at an early stage and challenging to treat when disease becomes advanced. Several oncolytic viruses (OVs) have been tested for ovarian cancer with modest results.

### What this study adds

► This is the first study offering a comprehensive immunological analysis of the immunogenic OV Orf virus (OrfV) in the context of preclinical ovarian cancer. OrfV treatment was particularly effective in controlling ascites fluid and secondary lesions in the peritoneal cavity when combined with tumor resection surgery. Efficacy relied primarily on effector natural killer (NK) cells, which expressed CXCR3 ligands and correlated with increased recruitment of T cells to the peritoneal cavity.

### How this study might affect research, practice or policy

► This study provides rationale for further study of immunogenic viruses that stimulate NK-cell responses and promote the CXCR3 signaling pathway to treat ovarian cancer. Investigating OrfV as a viral immunotherapy for ovarian cancer has the potential to strengthen the clinician's toolbox, particularly given its ability to potently activate the immune system.

## BACKGROUND

Epithelial ovarian cancer (EOC) is the most lethal gynecological malignancy.<sup>1</sup> The majority of EOC cases are diagnosed at an advanced stage, as early screening and detection methods are ineffective.<sup>2–4</sup> Standard of care therapy has remained largely unchanged and generally entails primary tumor cytoreductive surgery in

combination with taxane and platinum chemotherapy.<sup>5 6</sup> Patients with EOC develop ascites which contains tumor cells that can access organs housed in the abdomen and initiate fatal secondary lesions, making ascites control a primary target for novel therapies.<sup>7</sup>

Oncolytic viruses (OVs) are a promising multimodal immunotherapy platform.<sup>8</sup> OVs encompass a phylogenetically diverse cohort of viruses that have an inherent or engineered tropism for tumor cells.<sup>9</sup> OV infection of the tumor microenvironment (TME) kick-starts a proinflammatory immune response that ultimately clears the virus but also targets tumors for immune-mediated killing by innate and adaptive mechanisms.<sup>10 11</sup> To date, multiple OVs have crossed into clinical testing for ovarian cancer, including measles virus (clinicaltrials.gov, NCT00408590), reovirus (NCT01274624), herpesvirus (NCT03663712), adenovirus (NCT00964756), and vaccinia virus (VACV) (NCT02759588), demonstrating the anticipated potential of OVs for ovarian cancer.

Natural killer (NK) cells are innate cytotoxic lymphocytes adept at eliminating tumor cells and virus-infected cells. NK-cell targeting is not classically antigen-restricted but relies on a repertoire of activating and inhibitory receptors and cytokine signaling, making NK cells a promising effector subset to engage using antigen-agnostic immunotherapies.<sup>12 13</sup> NK-cell infiltrates in human tumor tissue correlate with enhanced survival in multiple cancer types, and antitumor NK responses can be modulated by immune checkpoint blockade.<sup>14 15</sup> Apart from their cytotoxic activity, NK cells crosstalk with type 1 classical dendritic cells (cDC1) and T cells during immune responses.<sup>16 17</sup> In melanoma, cDC1s are the dominant antigen-presenting cell that cross-presents tumor antigen to cytotoxic T lymphocytes (CTLs) to initiate tumor control.<sup>18</sup> cDC1s are recruited to the TME by NK cells, and the presence of NK cells and cDC1s are predictive of improved survival outcomes in numerous cancers.<sup>19 20</sup> The interaction between NK cells and cDC1s may be a promising axis of the immune response to target with OV therapy because this interaction regulates the stimulation of NK-cell and CTL responses, both of which are potent antitumor effectors.

*Parapoxvirus ovis* (Orf virus (OrfV)) is an oncolytic poxvirus that normally infects ungulates. OrfV is phylogenetically distinct from the oncolytic Chordopoxvirinae VACV, which has been extensively studied in preclinical and clinical settings and successfully combined with immune checkpoint blockade (ICB) in preclinical models of ovarian cancer.<sup>21</sup> OrfV is lytic in human cancer cells of diverse cellular origin and is effective against melanoma and colon cancer in preclinical mouse models, mainly through the potent stimulation of antitumor NK cells.<sup>22</sup> The capacity for OrfV to activate NK cells was exploited in a model of surgery-induced immune suppression, where OrfV therapy prevented NK-cell suppression and controlled metastatic tumor spread.<sup>23</sup> Given the broad oncolytic activity of OrfV and its ability to activate the immune

system, we hypothesized that OrfV would be an effective immunotherapy for ovarian cancer.

In this study, we demonstrate that OrfV and VACV are oncolytic against human and murine ovarian cancer cells. However, OrfV was a superior immunotherapeutic to VACV in vivo in our preclinical murine model of advanced-stage EOC. OrfV-mediated efficacy is reliant on tumoricidal NK cells that are supported by cDC1s and produce CXCR3 ligands to recruit CD8<sup>+</sup> T cells to the TME. This cross-talk between NK cells and dendritic cells (DCs) is evident in human ovarian cancer based on transcriptomics data, and notably, correlates with better patient outcomes. Finally, OrfV intervention can be combined with primary tumor removal surgery for optimal survival benefit. OrfV is a promising NK cell-stimulating immunotherapeutic platform with impressive efficacy against advanced-stage EOC.

## METHODS

### Mice

Seven-week-old female C57BL/6 mice (Charles River) and *Batf3* knockout mice (Jackson Laboratory, strain code #013755) were housed four to a cage in the Isolation Unit at the University of Guelph. Mice were acclimatized to the facility for 1 week prior to experimentation.

### Cell lines

ID8 transformed murine ovarian surface epithelial cells were generously donated by Drs K Roby and P Terranova (Kansas State University). HeLa, CAOV-3, Vero cells (ATCC CCL-2, HTB-75, and CCL-81, respectively), and ID8 cells were cultured in Dulbecco's High-Glucose Modified Eagle's Medium (DMEM) containing 10% fetal bovine serum (FBS). Human iOVCa147 cells were generously provided by Gabriel DiMattia (London Health Sciences Center) and were cultured in DMEM and Ham's F12 mixture (DMEM/F12). Sheep skin fibroblasts were cultured in DMEM containing 10% FBS. All cell lines were cultured in a humidified incubator at 5% CO<sub>2</sub> and 37.0°C and were confirmed to be mycoplasma-free prior to use (MycoAlert PLUS detection kit, Lonza).

### Viruses

OrfV-NZ2 (OrfV) was kindly provided by Dr Andrew Mercer (University of Otago), and vaccinia (Copenhagen strain, VVΔTK-GFP) was kindly provided by Dr John Bell (OHRI). OrfV was produced and titrated by 50% tissue culture infectious dose (TCID<sub>50</sub>) assay on SSF cells as described.<sup>24</sup> VACV was propagated on HeLa cells using methods similar to OrfV production.<sup>24</sup> VACV was titrated by TCID<sub>50</sub> assay on HeLa cells.

### Cell viability assays

Viral oncolysis of murine ID8 and human CAOV-3 and iOVCa147 cancer cell lines was performed by metabolic assay. 1e+04 cancer cells were seeded into 96-well plates and treated with OrfV or VACV at a range of multiplicities

of infection (MOIs) for 48 hours and incubated at 37°C and 5% CO<sub>2</sub>. Resazurin sodium salt (Sigma-Aldrich) was added at 0.5 mg/mL for 2 hours before data acquisition by fluorescent plate reader (excitation wavelength: 535/25 nm, emission wavelength: 590/35 nm). Relative metabolic activity was calculated by dividing fluorescent output of treatment cells by untreated control cells.

### Multistep virus growth curves

The capacity for ID8, CAOv-3, and iOVCa147 cancer cells to produce infectious OrfV and VACV particles was examined by multistep growth curves. Cancer cells were seeded at a density of 5e+05 cells per well in six-well plates and were infected with OrfV or VACV at an MOI=0.5. Virus from cells and supernatant were collected at a range of time points from 8 to 120 hours. Virus was released from infected cells by freeze–thaw and titrated by TCID<sub>50</sub> on SSFs and Vero cells for OrfV and VACV, respectively. TCID<sub>50</sub> values were converted to plaque-forming units (PFUs) by multiplying by 0.69, as previously described.<sup>25–27</sup>

### ID8 ascites-derived cell lines

Mice bearing ID8 ovarian tumors were monitored until their abdomens were distended from ascites fluid accumulation. Mice were then euthanized and ascites fluid was collected through insertion of a 25-gage needle in to the peritoneal cavity. Ascites fluid was immediately transferred into a heparinized tube to prevent clotting. Red blood cells were removed using ACK (ammonium-chloride-potassium) lysis buffer, and cells were pelleted by centrifugation at 500×g for 5 min at 4°C. Cell pellets were then resuspended in Roswell Park Memorial Institute (RPMI) 1640 with 10% FCS and plated in T75 flasks and incubated at 37°C and 5% CO<sub>2</sub>. Cells were grown until 90%–95% confluency and then expanded to T175 flasks and subsequently frozen to generate stocks at passage 2 and 3. All tests were conducted with ID8 ascites-derived cells at lower than passage 5.

### Orthotopic ID8 cancer model and standard virus therapy

The syngeneic orthotopic ID8 ovarian cancer model was set up as previously described.<sup>28</sup> Briefly, 1e+06 ID8 cells were injected into the left ovarian bursa of 7-week-old female C57BL/6 or Batf3 knockout mice. At 60 days following challenge, mice presented with signs similar to advanced-stage 3 EOC, including a large primary tumor, development of ascites in the peritoneal cavity, and secondary lesions on the peritoneum walls and other organs within the peritoneal cavity. For OrfV or VACV treatment, ID8 tumor-bearing mice were treated 60 days following tumor challenge with either virus at a dose of 5e+07 PFU delivered by intravenous or intraperitoneal injection, depending on the experiment. For experiments testing tumor burden reduction at 36 hours and 30 days following OrfV or VACV treatment, viruses were given in single doses. Mice in all subsequent survival experiments were given three doses at 5e+07 PFU of each virus directly into the peritoneal cavity given every other day starting

on day 60. Endpoints were either at prescribed times postvirus administration or when mice reached endpoint criteria, including distended abdomen interfering with mobility, hunched fur, irregular breathing, or isolated behavior. Necropsies were performed to collect endpoint data, including the volume of ascites fluid, the weight of the primary tumor, and the number of secondary lesions in the peritoneal cavity, to a maximum count of 100 lesions.

### Flow cytometric analysis of immune responses

NK and tumor-specific CTL responses were quantified by flow cytometry on peripheral blood and peritoneal lavage fluid. For NK-cell responses, mice were non-lethally bled and subjected to peritoneal lavage 36 hours following virus delivery. Samples were collected in heparinized tubes to prevent clotting, and sample volumes were recorded to normalize data to per microlitre (blood) or per millilitre (lavage fluid) standard. Red blood cells were lysed using ACK lysis buffer, and leukocytes were suspended in RPMI 1640 media containing 10% FBS and 0.1% beta-mercaptoethanol. Leukocytes were incubated for 1 hour, then brefeldin A (eBiosciences, cat#00-4506-51) was added to capture cytokine release, and incubation was continued for another 4 hours. Unless otherwise indicated, antibodies were purchased from BioLegend. Fc receptors were blocked by incubating with anti-CD16/32 (cat#101320) for 15 min at 4°C. Leukocytes were then stained with surface antibodies including allophycocyanin (APC) anti-NK1.1 (cat#108710), PE anti-programmed death-ligand 1 (PD-L1) (cat# 124308), fluorescein isothiocyanate (FITC) anti-CD69 (cat#104506), PE-Cy7 anti-CD27 (cat# 124215), PerCP5.5 anti-PD-1 (cat#109120), BV510 anti-CD8a (cat#100752), BV421 anti-CD3e (cat#100336), and BV421 anti-CD11b (eBiosciences, cat# 48-0112-82) for 20 min at 4°C in the dark. Fluorescence-activated cell sorting (FACS) buffer was then exchanged for phosphate-buffered saline (PBS), and leukocytes were stained for viability using the Zombie NIR (cat#423106) viability kit, following the manufacturer's protocol. Leukocytes were then treated with fixation buffer (cat#420801) and permeabilization buffer (cat#421002) and stained for intracellular interferon gamma (IFN-γ) with PE anti-IFN-γ (cat#505808), and granzyme B with FITC antigranzyme B (cat# 515403) for 20 min at 4°C in the dark. Cells were washed and suspended in 200 μL FACS buffer for flow cytometry analysis. Tumor-specific CTL responses were quantified as previously described.<sup>29</sup>

### Antibody depletion studies

C57BL/6 mice were challenged with 1e+06 ID8 cells into the left ovarian bursa to establish ovarian epithelial cancer. To deplete specific immunological cell subsets, depletion antibodies were delivered intraperitoneally 3 days and 1 day prior to virus administration on day 60, and then once per week to maintain depletion. The depletion antibodies and the initial depletion dose used in this study include anti-CD8a (BioXcell,



cat#BE0061 clone 2.43, 200 µg), anti-Thy1.2 (BioXcell, cat#BE0066 Clone 30H12, 200 µg) and Ultra-LEAF anti-asialo-GM1 (Biolegend, cat#146002, 50 µL). Depletions were confirmed by flow cytometry of peripheral blood on the day of virus treatment using the following antibodies: FITC anti-CD90.2 (BD Biosciences, cat#553013), PE anti-CD49b (DX5, BD Biosciences, cat#553858), BV510 anti-CD8a (BioLegend, cat#100752) and BV421 anti-CD3e (BioLegend, cat#100336).

### Tumor-directed antibody responses

Tumor-directed antibody responses were quantified as previously described.<sup>30</sup> Tumor-directed antibody data were analyzed by first subtracting background fluorescent of control wells from each sample. Then a curve was constructed for each sample using the dilution series. The area under the curve was then calculated for each sample and graphed alongside tumor-bearing but untreated animal controls.

### International Cancer Genome Consortium (ICGC) data set

Previously generated RNA-sequencing alignment data from human ovarian tumors was retrieved from the ICGC using score client. Ninety-two samples were used from 71 donors encompassing 64 primary, 25 recurrent and 3 metastatic tumors. All samples were retrieved with their associated clinical data. These alignment files were produced using the human reference genome (GRCh37) via STAR as described by the ICGC. HTseq (V.0.9.1, options: -m intersection-non-empty -i gene\_id -r pos -s no) was used to count reads over annotated genes.<sup>31</sup> Due to the robust normalization offered by DESeq, the raw counts produced by HTseq were normalized via DESEQ2\_normalize (V.3.8).<sup>32,33</sup> Previously established gene expression signatures were used to gage NK, cDC1s, CD8<sup>+</sup> T and B immune cell activity in the tumors.<sup>18,19,34</sup> For correlations between gene expression signatures, gene expression was log transformed ( $\log_2(1+\text{normalized expression})$ ).

### RNA sequencing

ID8 tumor-bearing animals were treated with a single dose of OrfV or PBS 60 days after tumor implantation. Peritoneal lavages were conducted 36 hours following virus. NK cells were enriched using a negative NK-cell isolation kit (Biolegend, cat#480049) and RNA was isolated using TRIzol (Thermo Fisher). Next-generation sequencing was conducted by Novogene. All fastq files were inspected with FASTQC, before HISAT2 alignment (V.2.0.0, -dta -no-mixed -no-discordant -no-unal) to a reference consisting of the entire mouse (V.GRCm38) and OrfV (V.1.21) genomes combined (online supplemental table 1). Samtools was then used to remove low-quality alignments ( $q < 1$ ) before running StringTie (1.3.4d, -e) to assemble and count transcripts based on mouse and ORF gene annotations. DESeq2 (default settings, R V.3.4.0) was used to normalize expression counts and determine differential gene expression between OrfV and untreated control groups. The differential gene expression volcano

plot and heat map were generated in GraphPad Prism. Gene ontology (GO) analysis was conducted using Panther V.16.0.

### PD-L1 expression and anti-PD-1 treatment

To assess PD-L1 expression, ID8 tumor cells were plated at  $5 \times 10^5$  cells per well in six-well plates and were incubated overnight. Cells were then treated with OrfV or VACV at an MOI=5 for 6 hours or were left untreated. ID8 cells were then gently released from the plate by incubating in 5 mM EDTA-PBS for 5 min. Cells were collected, centrifuged at  $500 \times g$  for 5 min and resuspended in FACS buffer. Fc receptors were blocked by incubating with anti-CD16/32 for 15 min at 4°C. Cells were then stained with PE anti-PD-L1 antibody (Biolegend, cat#124308) and 7AAD viability stain (Biolegend, cat#420404) for 20 min at 4°C in the dark before analysis by flow cytometry.

For anti-PD-1 ICB therapy combination treatment, ID8 tumor-bearing mice were treated with three doses of  $5 \times 10^7$  PFU of OrfV or VACV given every other day starting on day 60 post-tumor challenge. Anti-PD-1 (BioXcell, cat#BE0146) was delivered the day after the final dose of virus at 200 µg per dose into the peritoneal cavity. Anti-PD-1 treatments were continued every 3 days for a total of six treatments, and mice were monitored for survival.

### Primary tumor removal surgery

To model cytoreduction surgery commonly used to treat patients with human ovarian cancer, mice were challenged with  $1 \times 10^6$  ID8 cancer cells to the left ovarian bursa. At 60 days post-tumor challenge, mice with significant primary tumors and the start of ascites were anesthetized and primary tumors were surgically removed. Mice were allowed to recover for 48 hours following surgery, and OrfV treatment was initiated on day 62 following tumor challenge. Groups that did not receive primary tumor removal surgery were also treated with OrfV on day 62.

### DC culture experiments

Naïve C57BL/6 mice were euthanized, and bone marrow was collected from the femur and tibia bones by flushing with PBS.  $1 \times 10^6$  bone marrow-derived cells were cultured in RPMI 1640 medium containing 10% heat-inactivated FBS, 0.1% beta-mercaptoethanol and penicillin/streptomycin per 25 cm<sup>2</sup> cell culture flask. Initially, all cultures received 20 ng/mL of granulocyte-macrophage colony-stimulating factor (GM-CSF) on day 0 in 5 mL complete RPMI 1640. On day 2, an additional 5 mL of RPMI 1640 was added with 20 ng/mL of GM-CSF, and 10 ng/mL of interleukin (IL)-4 for a total of 10 mL. Half of the culture medium was removed on day 5 and replaced with new RPMI 1640 and cytokines. All cells were cultured at 37°C in a humidified atmosphere with 5% CO<sub>2</sub>. On day 7, non-adherent and loosely adherent cells were collected by gentle pipetting of the medium. DCs were counted and plated in 12-well plates at  $4 \times 10^5$  cells per well. Immediately following plating, DCs were treated with various



stimuli, including lipopolysaccharides (LPS) (100 ng/mL), naked OrfV (4e+06 PFU per well) and 100  $\mu$ L of cell-free supernatant from 4e+05 ID8 cells infected with an MOI=10 of OrfV for 6 hours. Two-hours following treatment, cells were treated with brefeldin A to capture cytokines and were then incubated for an additional 14 hours. Cultures were collected and stained for flow cytometry using the following surface antibodies: FITC anti-F4/80 (eBiosciences, cat#11-4801-85), PE/Cy7 anti-CD11c (BioLegend, cat#117318), APC/Fire750 anti-I-A/I-E (BioLegend, cat#107652), and BV421 anti-CD11b (BioLegend, cat#101236). Cell viability was assessed using the Zombie Aqua (BioLegend, cat#423102) viability kit, following the manufacturer's protocol. Cells were fixed and permeabilized as previously described, and then stained for intracellular cytokines using PE antitumor necrosis factor alpha (TNF- $\alpha$ ) and APC anti-IL-12. DCs were classified as CD11c<sup>+</sup> major histocompatibility complex (MHC)-II<sup>+</sup> F4/80 cells and were assessed for the proportion and mean fluorescent intensity of IL-12.

### Immunohistochemistry

At 60 days post tumor challenge, the left ovaries of C57BL/6 mice were removed following a small midline dorsal incision under isoflurane anesthesia. Ovaries were fixed in 10% neutral formalin overnight and washed with 70% ethanol for 24 hours. Tissues were processed through ethanol dehydration followed by clearing with xylene and embedding in paraffin wax using an automated processor. Tissues were serially sectioned (5  $\mu$ m) using a rotary microtome and mounted on charged slides (Superfrost Plus, Fisher Scientific) before being baked overnight at 37°C. Tissue sections were stained with H&E and visualized by a polarizing light microscope (E600-POL; NIKON, Toronto, Canada) at  $\times$ 20 magnification using Qcapture software.

### Statistical analyses

GraphPad Prism V.7 for Windows (<https://www.graphpad.com/>) was used for all graphing and statistical analyses. Survival curves were determined by the Kaplan-Meier method, and differences between groups were queried using the log-rank Mantel-Cox test. Immune response data, which involved one variable, were assessed by one-way analysis of variance (ANOVA) with Tukey's multiple comparisons test. Resazurin dye-based data, which involved two variables, were assessed by two-way ANOVA with Tukey's multiple comparisons test. All reported p values were two-sided and were considered significant at a p value of  $\leq$ 0.05. Graphs show means and SEs.

## RESULTS

### OrfV and VACV are oncolytic in murine and human ovarian cancer cell lines in vitro

The oncolytic activity of OrfV and VACV in murine (ID8) and human (CAOV-3 and iOVca147) ovarian cancer cells was assessed in vitro by metabolic assay at a range of MOIs.

OrfV killed ID8 cells better than VACV, but VACV outperformed OrfV in CAOV-3 and iOVca147 cells (figure 1A). Multi-step growth curve analyses revealed that ID8 cells supported replication of both OrfV and VACV, with VACV reaching titers over 2 logs higher than OrfV (figure 1B). In human CAOV-3 cells, OrfV did not replicate beyond the number of virus particles detected in the first 8 hours postinfection. There was a 4-log increase in the amount of infectious VACV particles from 8 hours to 24 hours. VACV replicated in iOVca147 cells, but OrfV did not. The enhanced killing and replicative ability of VACV within human ovarian cancer cells may be attributed to the enhanced tumor selectivity of VACV as a result of genetic thymidine kinase gene deletion. Despite variability in the production of new virus particles, both poxviruses were effective killers of murine and human ovarian cancer cell lines.

The immunotherapeutic potential of OrfV and VACV for ovarian cancer was tested using the immunocompetent orthotopic ID8 model, which has been used to test novel cancer therapeutics, including OVs.<sup>35 36</sup> Briefly, female C57BL/6 mice (n=8 per group) were challenged with ID8 cells implanted into the left ovarian bursa. After 60 days, mice presented with disease that mirrors advanced-stage EOC in humans, including a large primary tumor, accumulation of ascites fluid in the peritoneal cavity and dissemination of secondary lesions throughout the peritoneal cavity. ID8 tumor-bearing mice were treated with a single dose of 5e+07 PFU of OrfV or VACV delivered on day 60 post-tumor challenge, either directly to the peritoneal cavity (intraperitoneally) or intravenously (figure 1C). To standardize comparisons, we sacrificed cohorts of mice 36 hours and 30 days after the virus and measured the weight of the primary tumor and the volume of ascites recovered from the peritoneal cavity. At 36 hours following OV therapy, OrfV delivered by either injection route decreased primary tumor size compared with PBS-treated controls. In contrast, VACV did not have a significant effect on the primary tumor. OrfV reduced ascites compared with PBS-treated controls, as did VACV, but only when delivered intravenously. At 30 days following the virus, no reduction in the primary tumor weight was observed in any treatment group compared with control. However, OrfV delivered intraperitoneally significantly reduced ascites compared with both control mice and mice that received VACV. We derived three polyclonal primary tumor cell lines from the ascites of ID8 mice: ID8-ASC03, ID8-ASC04, and ID8-ASC12, and tested them in vitro for sensitivity to OrfV or VACV oncolysis. The ID8 ascites-derived cell lines were more sensitive than the parental ID8 cells to killing by OrfV but not to VACV (figure 1D). These data suggested that neither virus was capable of long-term control of the primary tumor, but that OrfV was effective at controlling ascites, especially when delivered directly to the peritoneal cavity.

To examine the impact of OrfV and VACV on survival outcome in the ID8 model of advanced EOC, ID8 mice

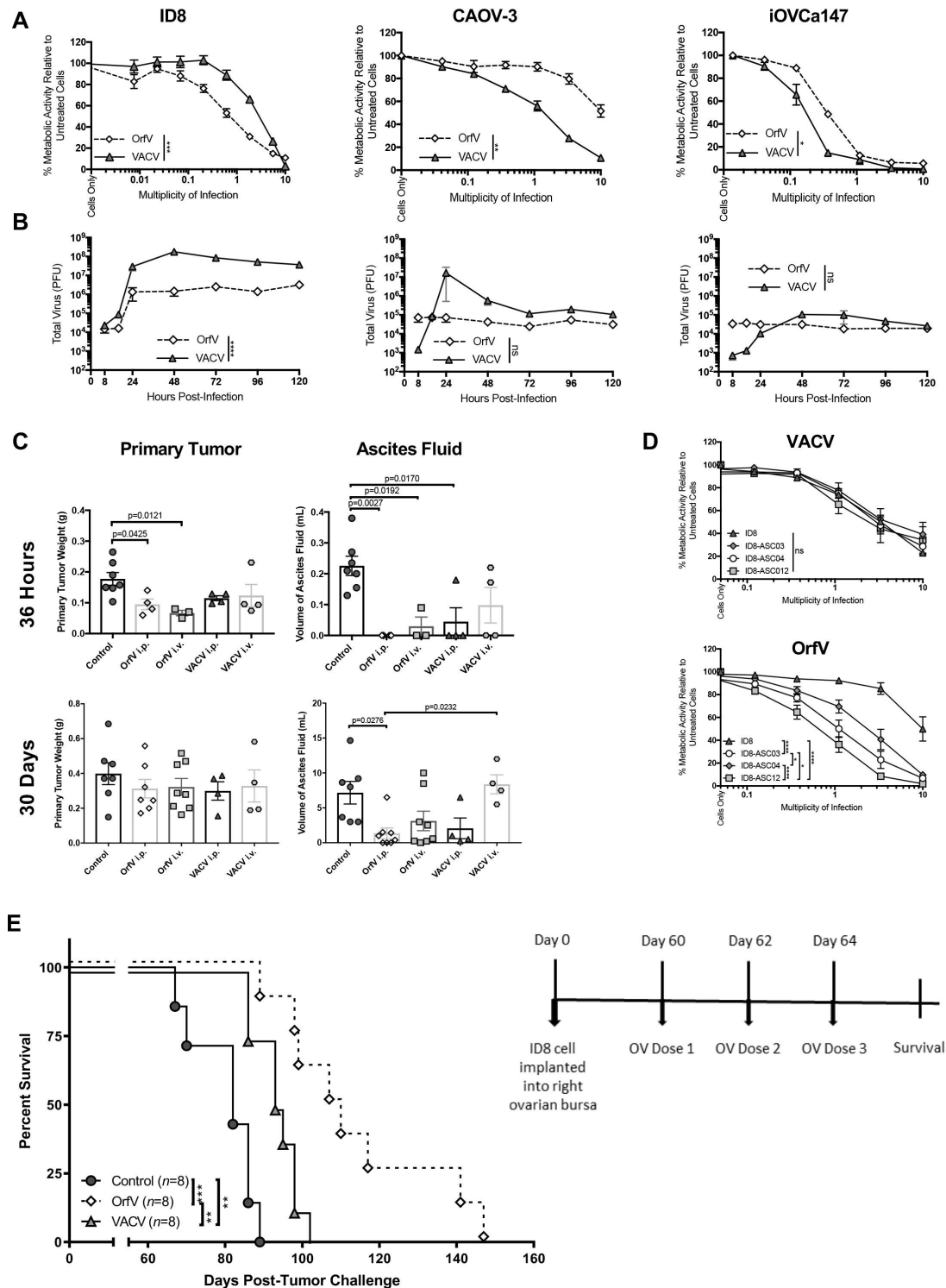


**Figure 1** OrV and VACV kill murine and human ovarian cancer cells and extend survival in a preclinical model of advanced EOC. (A) Mouse ID8 and human CAOV-3 and iOVCa147 ovarian cancer cells were infected with OrV or VACV at a range of MOI. Cell viability 72 hours after incubation was determined by resazurin metabolic activity assay. Statistical analysis was by two-way analysis of variance. (B) ID8, CAOV-3 and iOVCa147 cells were infected with OrV or VACV at an MOI of 0.5, and infectious virus was quantified over time by TCID<sub>50</sub>. (C) Mice bearing advanced ID8 EOC were treated with a single dose of OrV or VACV by intravenous or intraperitoneal injection. Thirty-six hours (top) or 30 days (bottom) after treatment, the weight of the tumor-bearing ovary (left) and the volume of ascites fluid (right) accumulated in the peritoneal cavity were quantified. (D) ASC03/04/12 and ID8 tumor cells were infected with either OrV (middle) or VACV (bottom) at a range of MOI. Cell viability 48 hours after infection was determined by metabolic activity assay. (E) Mice bearing advanced ID8 EOC were treated with 5e+07 PFU of OrV or VACV by intraperitoneal injection as per the schematic. Survival was assessed by log-rank test. \*P≤0.05, \*\*P≤0.01, \*\*\*P≤0.001, \*\*\*\*P≤0.0001. EOC, epithelial ovarian cancer; ns, not significant; MOI, multiplicity of infection; OrV, Orf virus; PFU, plaque-forming unit; VACV, vaccinia virus.

(n=8) were treated with three doses of  $5 \times 10^7$  PFU of either virus given every other day by intraperitoneal injection. Control animals had a median survival of 82 days following tumor challenge (figure 1E). Survival was enhanced by VACV therapy to a median survival of 94 days and an HR of 0.2737 compared with control animals. OrfV was more effective than VACV, leading to a median survival of 108.5 days and an HR of 0.2212 compared with control animals. Two animals treated with OrfV survived ~40 days longer than the last animal treated with VACV to reach the endpoint. These data indicated OrfV as a more potent platform than VACV in the ID8 model of advanced-stage EOC.

### **OrfV intervention for advanced-stage EOC extends survival, reduces the spread of secondary lesions and induces a robust anticancer effector immune response**

Since OrfV was more effective than VACV in our in vivo experiments, we decided to focus on elucidating the antitumor mechanisms of OrfV therapy. Survival experiments with multidose OrfV therapy delivered intraperitoneally were repeated three times to generate a comprehensive survival dataset (figure 2A). OrfV therapy extended survival to a mean of 109.5 days compared with 93 in control animals (HR=0.2859). In support of OrfV being particularly effective against ascites accumulation, peritoneal lavage fluid collected 10 days following OrfV was clear, in contrast to lavage fluid from control mice (figure 2B). Secondary lesions in the peritoneal cavity were reduced in OrfV-treated mice at endpoint ( $p=0.0025$ , figure 2C). Additionally, there were fewer cases of secondary lesions homing to the spleen in OrfV-treated animals compared with controls (figure 2D). Cumulatively, these data suggested that OrfV was effective at controlling ascites burden and disease spread in vivo by targeting tumor cells in the ascites fluid.

As multimodal therapeutics, OV directly kill cancer cells and stimulate host anticancer immune responses.<sup>37</sup> To determine the contribution of the host immune response to OrfV efficacy against advanced ID8 EOC, peritoneal lavages were performed 10 days following OrfV or PBS treatment for immune cell phenotyping by flow cytometry. OrfV treatment increased the number of CD4<sup>+</sup> and CD8<sup>+</sup> T cells in the peritoneal cavity (figure 2E). Using a coculture assay with interferon-stimulated ID8 cells, we observed recall responses from CD4<sup>+</sup> and CD8<sup>+</sup> T cells isolated from OrfV-treated mice but not control animals (figure 2F,G). Additionally, there were more CD4<sup>+</sup> T cells producing TNF- $\alpha$  in the peritoneal cavity of OrfV-treated mice than PBS controls (figure 2H). These data indicated that OrfV treatment can stimulate tumor-directed T-cell responses in the ascites TME.

OrfV is known to stimulate strong antitumor NK-cell responses.<sup>35</sup> To interrogate the NK-cell compartment, peritoneal lavages were conducted 36 hours post-OrfV treatment. The number of NK cells in the peritoneal cavity was increased by OrfV treatment (figure 2I), with increases in both CD11b<sup>+</sup> CD27<sup>-</sup> and CD11b<sup>+</sup> CD27<sup>+</sup>

NK-cell subsets (figure 2J). Further phenotyping of NK cells in the peritoneal cavity revealed an increase in NK cells expressing activation markers CD69 (figure 2K) and PD-L1 (figure 2L) and cytotoxic granzyme B (figure 2M). These observations confirmed that OrfV stimulates a robust NK-cell response in the ascites TME.

Immunological analyses were extended to include quantification of tumor-directed antibodies. Plasma was collected 21 days following the first dose of OrfV therapy. Therapy-induced antibodies were quantified by coincubation of diluted plasma samples with target ID8 cells and subsequent detection with a fluorescence-conjugated anti-mouse IgG secondary, as previously described.<sup>30</sup> An increase in serum-circulating therapy-induced antibodies was detected in OrfV-treated mice over control animals (figure 2N). The magnitude of the tumor-directed antibody response correlated with survival ( $R^2=0.4706$ ,  $p=0.0047$ ; figure 2O). Together, these data indicated that OrfV intervention stimulated responses from multiple anticancer effector subsets: NK cells, CD8<sup>+</sup> T cells, and antibodies.

### **Immune subset depletion revealed a critical role for NK cells and CD8 $\alpha$ <sup>+</sup> cells**

Given that NK and CD8<sup>+</sup> T cells responded to OrfV therapy, each was depleted in vivo and their impact on survival was measured. Mice that received OrfV but were depleted of NK cells by anti-asialo GM1 antibody had no survival advantage over control mice, supporting NK cells as a key driver of OrfV therapy (figure 3A). To investigate the functional role of T cells, CD8 $\alpha$ <sup>+</sup> cells were depleted using anti-CD8 $\alpha$  antibody, and CD8 $\alpha$ <sup>+</sup> and CD4<sup>+</sup> T cells were depleted simultaneously by injection of anti-Thy1.2 (CD90.2), which is a pan-T-cell marker.<sup>38</sup> The therapeutic effect of OrfV was blunted in mice receiving OrfV with CD8 $\alpha$ <sup>+</sup> cells depleted (figure 3B). In contrast, when T cells were depleted with anti-Thy1.2, an intermediate effect was observed that did not achieve statistical significance compared with either the OrfV or the control groups. These data indicated anti-CD8 $\alpha$ , which can deplete any cell expressing CD8 $\alpha$ , was more detrimental to OrfV therapeutic efficacy than depletion of both CD4<sup>+</sup> and CD8 $\alpha$ <sup>+</sup> T-cell subsets together by anti-Thy1.2. Taken together, NK cells were a dominant anticancer effector subset induced by OrfV therapy, and a CD8 $\alpha$ <sup>+</sup> cell subset extraneous to CTLs may play a supportive role.

### **NK cells and CD8 $\alpha$ <sup>+</sup> cDCs collaborate to mediate OrfV therapeutic efficacy**

cDC1s express CD8 $\alpha$ ,<sup>39</sup> are a major contributor to anti-tumor T-cell responses in vivo<sup>40</sup> and require the BATF3 transcription factor for development. Mice deficient in CD8 $\alpha$ <sup>+</sup> cDCs cannot generate adequate de novo anti-tumor T-cell responses and do not resist T cell-sensitive tumor outgrowth.<sup>18 41</sup> CD8 $\alpha$ <sup>+</sup> cDCs support NK cell-mediated control of tumor metastases by producing IL-12, and in return NK cells support cDC1 recruitment to the TME.<sup>20 42</sup> We hypothesized that OrfV stimulates



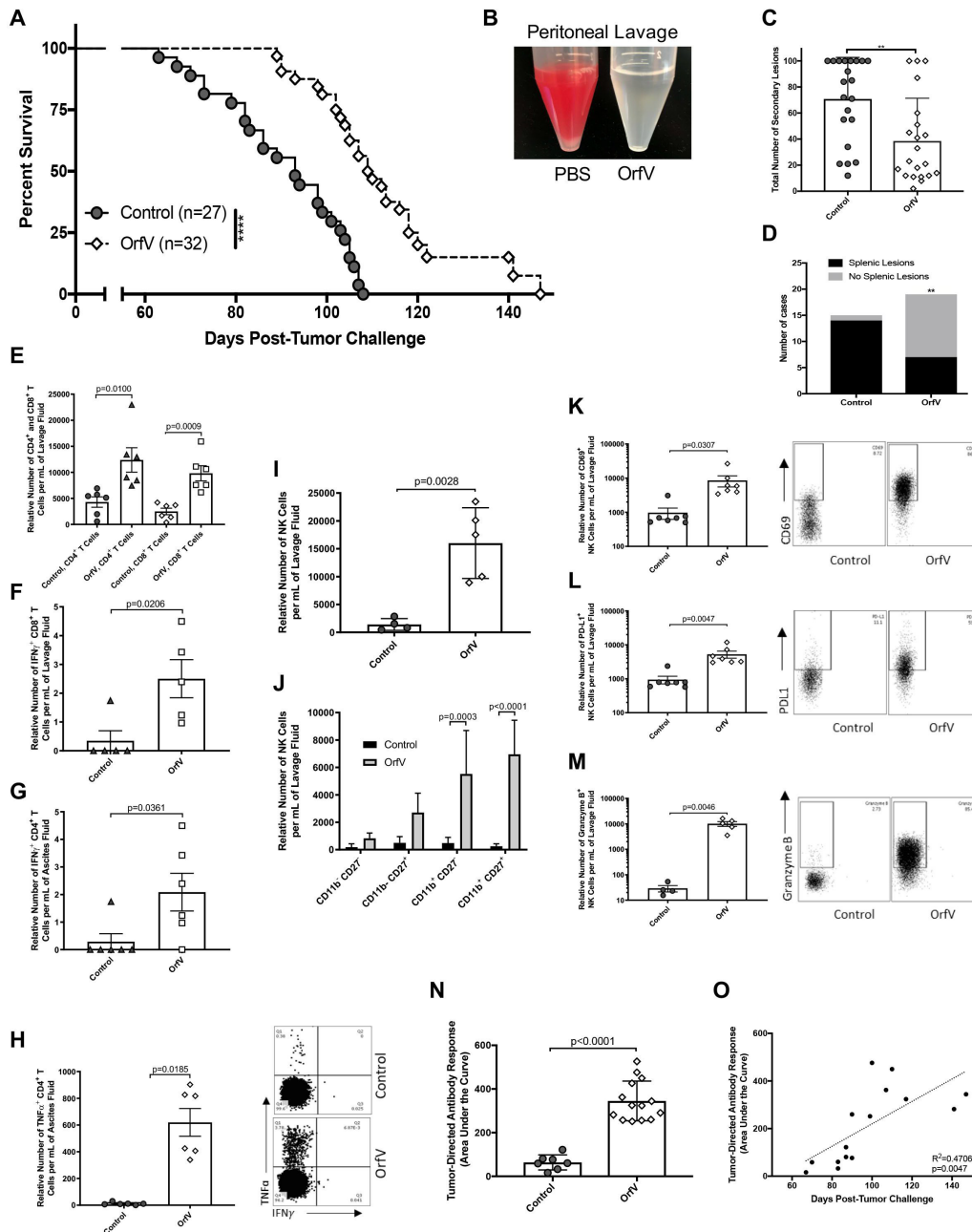


**Figure 2** OrfV reduces ascites burden and activates a robust multi-effector immune response to control advanced-stage EOC. (A) ID8 mice were treated with three doses of intraperitoneal OrfV starting on day 60. Survival was assessed by log-rank test. \*\*\*\*P<0.0001. (B) Peritoneal lavage fluid from ID8 mice ten days after treatment with PBS or a single dose of OrfV. (C) The number of secondary lesions in the peritoneal cavity at endpoint in mice treated with OrfV or PBS. (D) The number of secondary lesions on the spleen at endpoint in mice treated with OrfV or PBS. (E) Ten days after OrfV treatment, the number of CD4<sup>+</sup> and CD8<sup>+</sup> T cells in the peritoneal cavity of ID8 mice was quantified by flow cytometry. (F) The number of tumor-specific IFN- $\gamma$ <sup>+</sup> CD8<sup>+</sup> T cells in the peritoneal cavity of OrfV-treated ID8 mice was quantified by flow cytometry following coculture with IFN-stimulated target ID8 cells. (G) The number of tumor-specific IFN- $\gamma$ <sup>+</sup> CD4<sup>+</sup> T cells in the peritoneal cavity of OrfV-treated ID8 mice was quantified by flow cytometry following coculture with IFN-stimulated target ID8 cells. (H) The number of TNF- $\alpha$  expressing CD4<sup>+</sup> T cells in the peritoneal cavity 10 days following OrfV therapy was quantified by flow cytometry. (I) Three days after OrfV treatment of ID8 mice, the number of NK cells in the peritoneal cavity was quantified by flow cytometry. (J) The relative number of NK cells in the peritoneal cavity by maturation status was determined by CD11b and CD27 surface expression. (K) The number of NK cells expressing CD69 in the peritoneal cavity of ID8 mice 3 days after treatment. (L) The number of NK cells expressing PD-L1 in the peritoneal cavity of ID8 mice 3 days after treatment. (M) The number of NK cells expressing granzyme B in the peritoneal cavity of ID8 mice 3 days after treatment. (N) ID8 mice were bled 21 days after OrfV or PBS treatment and tumor-specific antibodies were quantified by immunofluorescence assay and expressed as area under the curve. (O) The magnitude of the anti-ID8 antibody response was compared with the duration of overall survival by bivariate correlation. \*\*\*\*P<0.0001. EOC, epithelial ovarian cancer; IFN, interferon; IFN- $\gamma$ , interferon gamma; NK, natural killer; OrfV, Orf virus; TNF- $\alpha$ , tumor necrosis factor alpha.

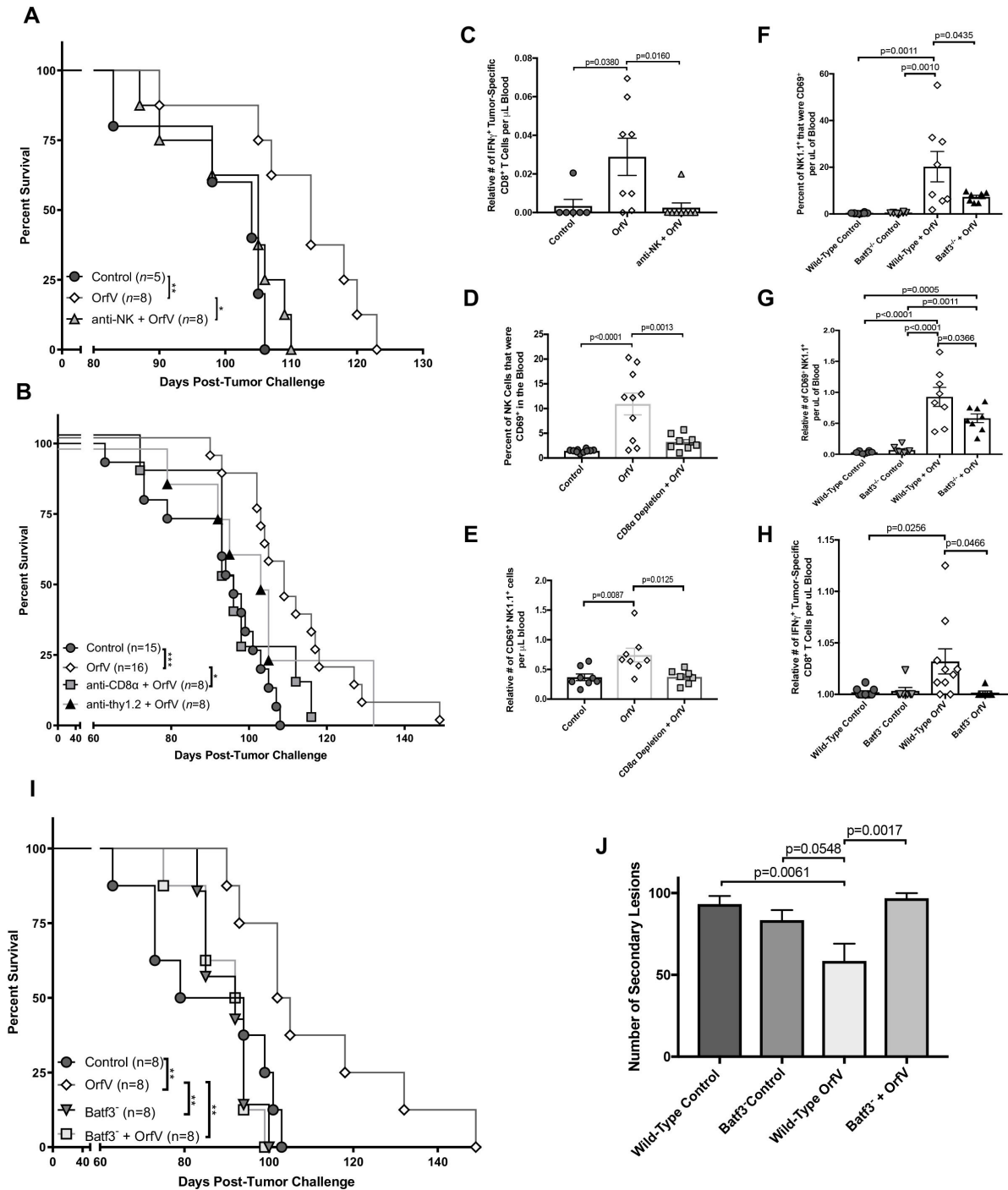


**Figure 3** NK cells are a dominant anticancer effector subset induced by OrfV and NK cells and CD8 $\alpha$ <sup>+</sup> cDCs collaborate to mediate OrfV therapeutic efficacy. (A) NK cells were depleted in vivo by anti-asialo antibody prior to OrfV treatment. Survival between groups was compared by log-rank test. (B) Anti-CD8 $\alpha$  or anti-thy1.2 was used to deplete T cells in vivo prior to OrfV treatment. Survival was assessed by log-rank test. (C) The number of IFN- $\gamma$ <sup>+</sup> CD8<sup>+</sup> T cells in the blood of ID8 tumor-bearing animals was quantified by coculture assay 10 days after treatment with PBS or OrfV, with or without NK depletion. (D) The proportion of CD69<sup>+</sup> NK cells recovered from the blood 36 hours after OrfV treatment in ID8 mice, with or without CD8 $\alpha$  depletion. (E) The number of CD69<sup>+</sup> NK cells recovered from the blood 36 hours after OrfV treatment in ID8 mice, with or without CD8 $\alpha$  depletion. (F) WT or Batf3<sup>-</sup> mice bearing ID8 tumors were treated with OrfV and 36 hours later the proportion of CD69<sup>+</sup> NK cells in the blood was determined. (G) WT or Batf3<sup>-</sup> mice bearing ID8 tumors were treated with OrfV and 36 hours later the number of CD69<sup>+</sup> NK cells in the blood was determined. (H) WT or Batf3<sup>-</sup> mice bearing ID8 tumors were treated with OrfV, and 10 days later, IFN- $\gamma$ <sup>+</sup> CD8<sup>+</sup> T cells were quantified in the blood. (I) ID8 tumor-bearing mice in the WT or Batf3<sup>-</sup> background were treated with OrfV. Survival comparisons were performed by log-rank test (left). (J) The number of secondary lesions populating the peritoneal cavity was counted on endpoint in ID8 tumor-bearing mice in the WT or Batf3<sup>-</sup> background treated with OrfV or PBS. \*P $\leq$ 0.05, \*\*P $\leq$ 0.01, \*\*\*P $\leq$ 0.001. cDC, classical dendritic cell; IFN- $\gamma$ , interferon gamma; NK, natural killer; OrfV, Orf virus; WT, wild type.

an inflammatory program wherein NK cells, cDC1s, and CTLs work in concert to control ID8 tumors. In line with this, a near-complete abrogation of tumor-specific CTL responses occurred when NK cells were depleted (figure 3C). Similarly, mice depleted of CD8a<sup>+</sup> cells had a decreased proportion (figure 3D) and relative number (figure 3E) of NK cells in circulation expressing the activation marker CD69. Furthermore, the cell-free supernatant from ID8 cells infected with OrfV in vitro stimulated IL-12 production from cultured DCs (online supplemental figure 1A,B). Therefore, NK and CTL responses following OrfV were closely linked, and OrfV-infected ID8 tumor cells were capable of inducing IL-12 production from DCs.

We hypothesized that the elimination of cDC1s would attenuate both NK and CTL responses, therefore reducing OrfV efficacy. To test this hypothesis, *Batf3*<sup>-/-</sup> knockout mice (n=8), which cannot develop cDC1s,<sup>39</sup> were challenged with ID8 tumor cells and treated at day 60 with OrfV therapy. Control *Batf3*<sup>-/-</sup> and wild-type mice were treated with PBS. Thirty-six hours following OrfV therapy, *Batf3*<sup>-/-</sup> mice had a reduced proportion (figure 3F) and relative number (figure 3G) of activated CD69<sup>+</sup> NK cells in circulation compared with wild-type mice. The magnitude of the tumor-specific CTL response was blunted in *Batf3*<sup>-/-</sup> mice compared with wild-type counterparts (figure 3H). *Batf3*<sup>-/-</sup> mice that received PBS did not differ in survival compared with wild-type control mice, and OrfV did not prolong survival in *Batf3*<sup>-/-</sup> mice. OrfV therapy in wild-type mice resulted in a median survival of 103.5 days, with one mouse surviving to the end of the experiment on day 140 without visible disease on necropsy (figure 3I). OrfV-treated *Batf3*<sup>-/-</sup> mice had a higher secondary lesion burden in the peritoneal cavity at endpoint compared with OrfV-treated wild-type mice (figure 3J). This corroborated previous evidence that cDC1s contribute to control of metastatic disease.<sup>42</sup> These data demonstrate that cDC1s play a central role in the anticancer immune response initiated by OrfV and are required for OrfV-mediated efficacy.

### Intratumoral NK-cell recruitment correlates with cDC1s and enhanced survival in human ovarian cancer

The data thus far have demonstrated that OrfV stimulates the immune system through NK cells and cDC1s to improve therapeutic outcomes. We next questioned whether the interplay we observed between NK cells, cDC1s and T cells exists and influences outcomes in human ovarian cancer. Of note, recent studies have demonstrated that NK cells recruit cDC1s to the TME in several human cancers, and that CCR7<sup>+</sup> cDC1s are critical for driving both NK-cell and CTL responses that correlate with improved overall survival.<sup>18–20</sup> Gene expression datasets from primary human ovarian tumors from the ICGC database were analyzed using previously published gene expression signatures for NK cells, cDC1s, CD8<sup>+</sup> T cells, and CD4<sup>+</sup> T cells<sup>19,34</sup> to evaluate the correlation between immune cell subsets in tumor tissue (figure 4A). Positive correlations

between NK cells and cDC1s ( $R^2=0.406$ , figure 4B), NK cells and CD8<sup>+</sup> T cells ( $R^2=0.5432$ , figure 4C), cDC1s and CD8<sup>+</sup> T cells ( $R^2=0.6311$ , figure 4D), and CD4<sup>+</sup> T cells and cDC1s ( $R^2=0.6630$ , figure 4E) were observed, suggesting that these cells interact in the ovarian TME. Transcriptomic data were binned based on the expression level of NK, cDC1, CD8<sup>+</sup>, and CD4<sup>+</sup> T-cell signatures, and the top and bottom thirds were analyzed for survival outcome. A high magnitude of NK cells in the TME correlated with increased overall survival (figure 4F). However, the magnitude of cDC1s, CD4<sup>+</sup>, and CD8<sup>+</sup> T cells did not yield a significant difference in overall survival in this dataset (figure 4F–I). Intriguingly, we observed a correlation between the cDC1 signature and a refined NK-cell signature comprising killer cell lectin-like receptor (KLRC or NKG2 family) genes including *KLRC1*, *KLRC2*, and *KLRC3*, which encode several receptors important in NK-cell regulation and function (figure 4J). The magnitude of KLRC gene expression positively correlated with overall survival (figure 4K), which has been demonstrated in melanoma.<sup>19</sup> These analyses suggest that NK cells are predictive of survival and that therapies, like OrfV, that boost NK-cell function may be translatable to human ovarian cancer.

### Transcriptomics of NK cells enriched from the ascites TME

To better understand of the role of NK cells in OrfV therapy, NK cells were collected by peritoneal lavage of mice 36 hours after treatment. NK cells were enriched using a negative bead selection kit and the transcriptome was analyzed by RNA sequencing. A total of 3274 differentially expressed genes were detected with 1736 upregulated and 1538 downregulated in the OrfV-treated groups relative to PBS (figure 5A). GO analysis showed an enrichment in genes involved in host defense response, immune system process, and response to cytokine (figure 5B). The top 50 differentially expressed genes (by adjusted p value, figure 5C) included genes involved in response to type 1 IFN- $\gamma$  and cytokine production and included the cytolytic granzymes B and C. An analysis of genes encoding NK cell activating and inhibitory receptors, as well as activation markers, revealed an increase in *Klra1*, *Klra3*, *Klra7*, and *CD69*, along with a dramatic upregulation of *CD274* (PD-L1, figure 5D). As NK cells can regulate the response of other immune cells using cytokines, a focused analysis on cytokine gene expression was conducted. Following OrfV therapy, NK cells upregulated proinflammatory cytokines (figure 5E), including *IL-27*, *IL-15* and *IL-6*, and *CXCL10*, *CCL24*, *CXCL9*, and *CXCL11*. These data indicate that enriched NK cells isolated from the ascites TME rapidly respond to OrfV by inducing a complex multi-gene expression program that includes genes involved in host defense and response to pathogen, and that NK cells express cytokines and chemokines that may be critical for a robust antitumor immune response.



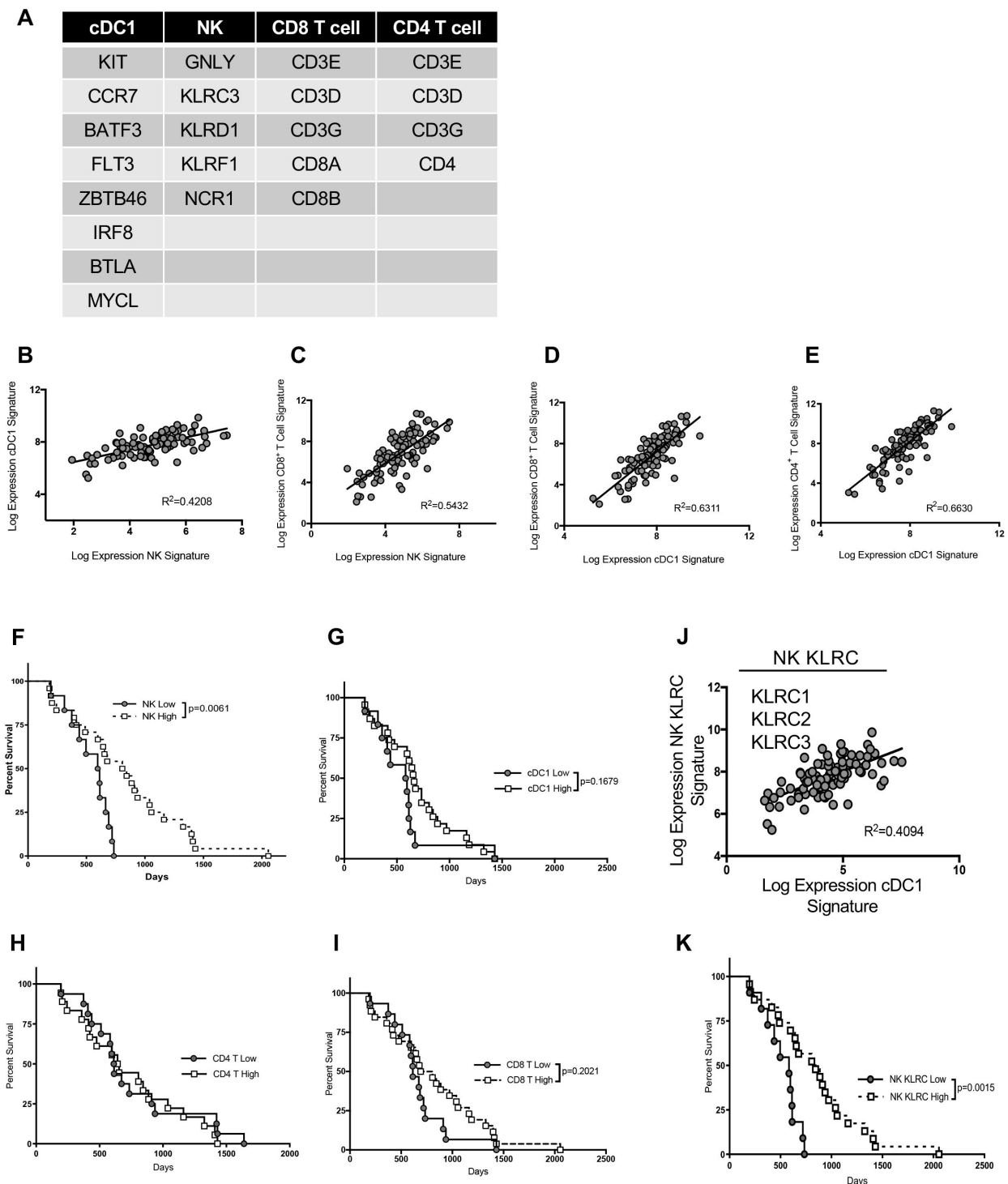


**Figure 4** NK cells correlate with cDC1s and T cells in the human ovarian TME and are linked to better overall survival. (A) Gene signatures used to identify cDC1, NK, CD8<sup>+</sup> and CD4<sup>+</sup> T cells from the ICGC human ovarian cancer dataset. (B) Bivariate correlation comparing cDC1s and NK cells in the ICGC human ovarian cancer dataset. (C) Bivariate correlation comparing CD8<sup>+</sup> T cells and NK cells in the ICGC human ovarian cancer dataset. (D) Bivariate correlation comparing CD8<sup>+</sup> T cells and cDC1s in the ICGC human ovarian cancer dataset. (E) Bivariate correlation comparing CD4<sup>+</sup> T cells and cDC1s in the ICGC human ovarian cancer dataset. (F) Log-rank test of ICGC patient samples binned according to the highest and lowest thirds of NK-cell signature expression. (G) Log-rank test of ICGC patient samples binned according to the highest and lowest thirds of cDC1-cell signature expression. (H) Log-rank test of ICGC patient samples binned according to the highest and lowest thirds of CD4<sup>+</sup> T-cell signature expression. (I) Log-rank test of ICGC patient samples binned according to the highest and lowest thirds of CD8<sup>+</sup> T-cell signature expression. (J) Bivariate correlation comparing the KLRG NK-cell signature and the cDC1 signature in the ICGC human ovarian cancer dataset. (K) Log-rank test of ICGC patient samples binned according to the highest and lowest thirds of KLRG1 NK-cell signature expression. cDC1, classical type 1 dendritic cell; ICGC, International Cancer Genome Consortium; KLRC, killer cell lectin-like receptor; NK, natural killer; TME, tumor microenvironment.

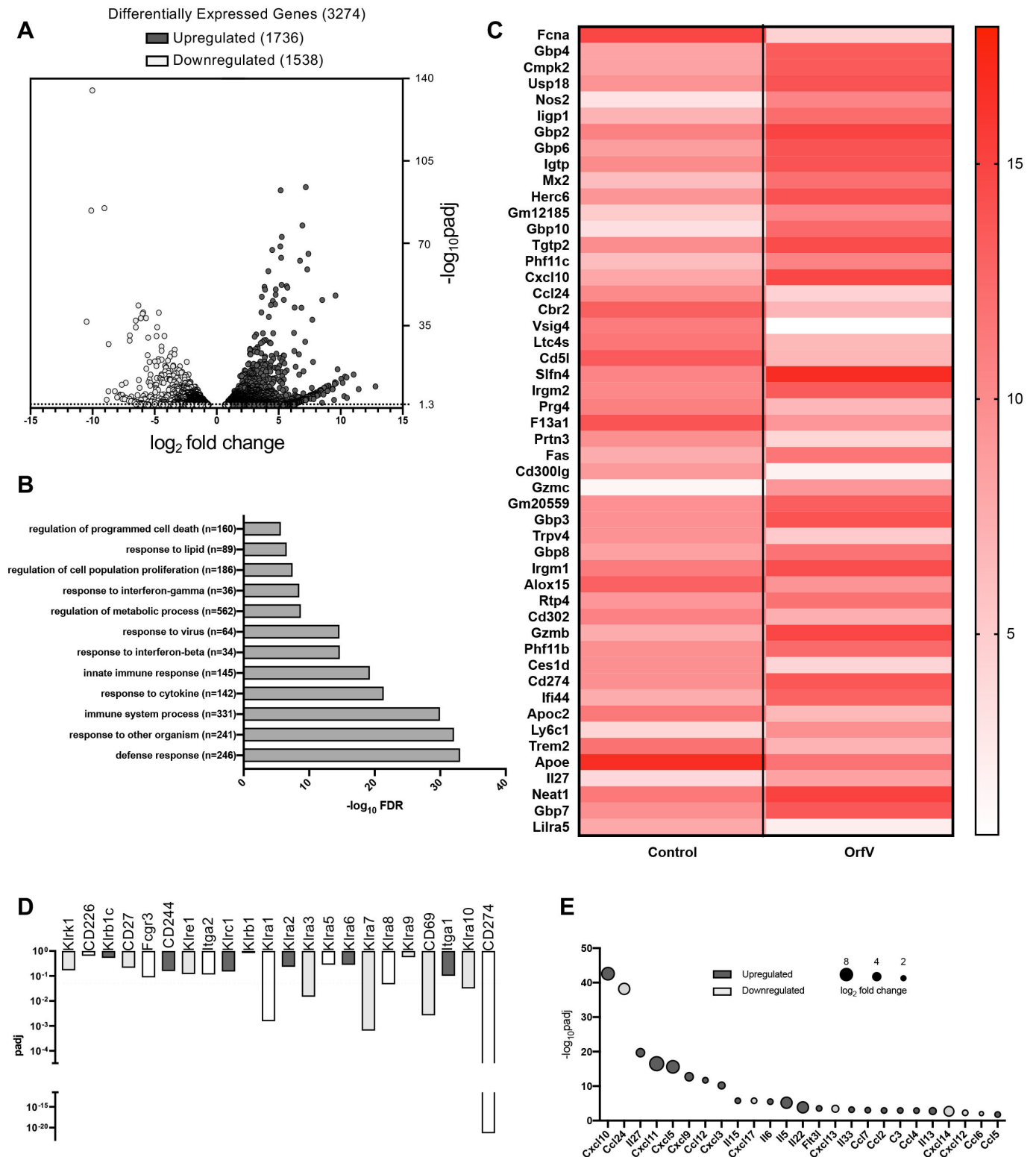


**Figure 5** NK cells enriched from the ascites TME express an antiviral and proinflammatory transcriptional program. (A) Genes differentially expressed between NK cells enriched from the peritoneal cavity of ID8 tumor-bearing treated with OrfV compared with PBS are represented by volcano plot. (B) GO analysis of differentially expressed genes was conducted using Panther analysis. Twelve of the most enriched GO terms from biological process are shown with the number of genes enriched in each category. (C) Heat map of 50 of the top differentially expressed genes in enriched NK cells. Shading represents the magnitude of averaged normalized gene expression. (D) The adjusted p values of NK receptors and activation markers comparing NK cells enriched from the peritoneal cavity of control and OrfV-treated mice. (E) The enriched NK transcriptomics dataset was interrogated for differential expression of cytokines and chemokines and represented graphically by adjusted p value (y-axis), direction of differential expression (gray, upregulated; white, downregulated) and fold change (size of data points). GO, gene ontology; NK, natural killer; OrfV, Orf virus.

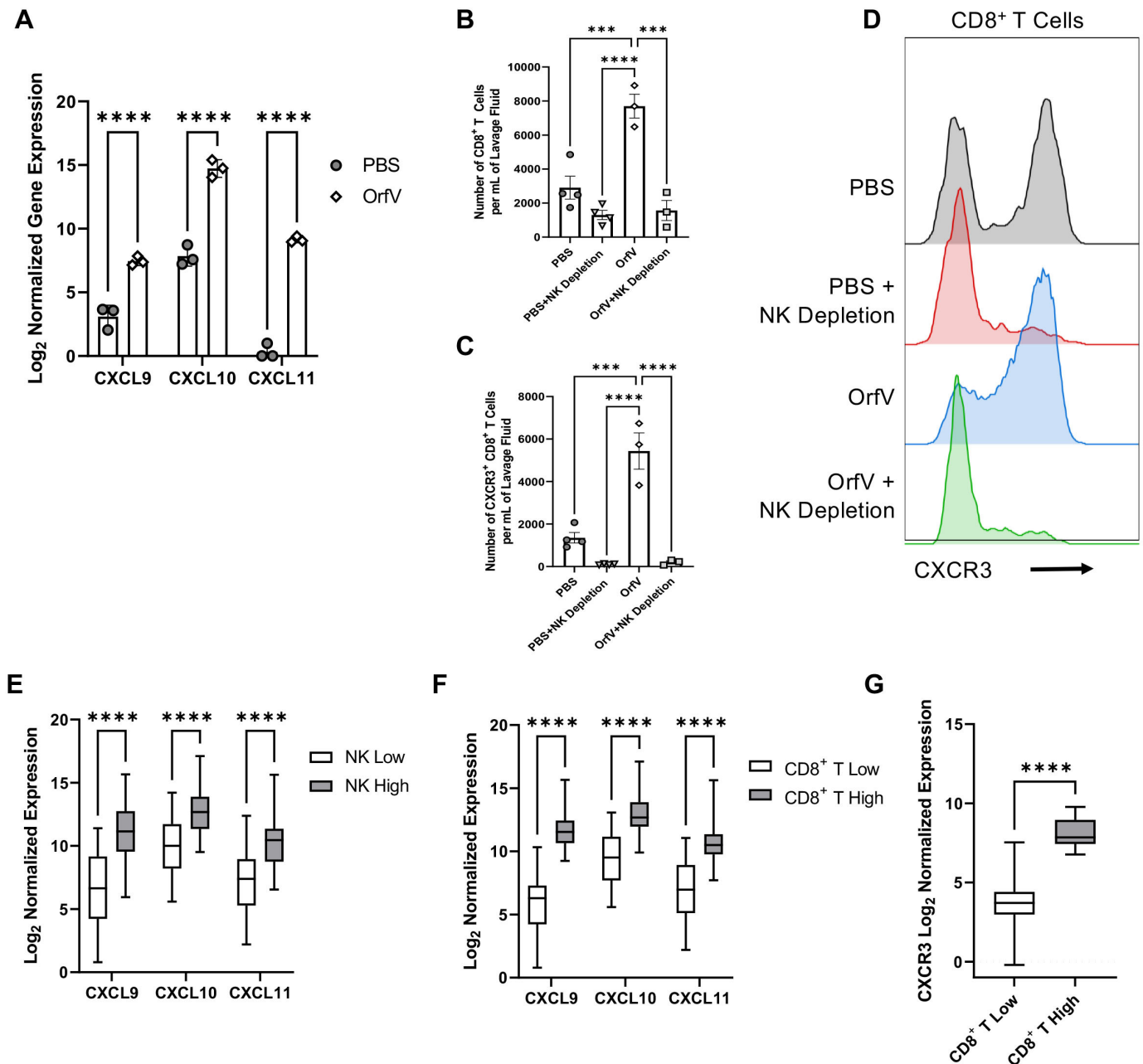


**Figure 6** OrV recruits immune effector cells via the CXCR3 pathway. (A) The enriched NK transcriptomics dataset was interrogated for CXCL9, CXCL10, and CXCL11. The normalized expression of each from PBS or OrV-treated mice is shown. (B) The number of CD8<sup>+</sup> T cells was determined per millilitre of peritoneal lavage fluid in mice treated with OrV with or without NK-cell depletion. (C) The number of CD8<sup>+</sup> T cells expressing CXCR3 was determined per millilitre of peritoneal lavage fluid in mice treated with OrV with or without NK-cell depletion. (D) Histograms of the expression of CXCR3 on CD8<sup>+</sup> T cells isolated from the peritoneal lavage fluid of mice treated with OrV with or without NK-cell depletion. (E) The ICGC human ovarian cancer dataset was interrogated for the expression of CXCL9, CXCL10, and CXCL11 in high and low NK-cell gene signature samples. (F) The ICGC human ovarian cancer dataset was interrogated for the expression of CXCL9, CXCL10, and CXCL11 in high and low CD8<sup>+</sup> T-cell gene signature samples. (G) The ICGC human ovarian cancer dataset was interrogated for the expression of CXCR3 in high and low CD8<sup>+</sup> T-cell gene signature samples. \*\*\* $P \leq 0.001$ , \*\*\*\* $P \leq 0.0001$ . ICGC, International Cancer Genome Consortium; NK, natural killer; OrV, Orf virus.

### NK cells regulate T-cell recruitment in ovarian cancer through the CXCR3 chemokine axis, which is accentuated by OrV therapy

The highest upregulated gene from the cytokine focused transcriptomics analysis was the CXCR3 ligand CXCL10 (figure 5E). CXCR3 has two additional ligands, CXCL9

and CXCL11, which were also upregulated in OrV-treated enriched NK cells (figure 6A). We hypothesized that NK cells regulate T-cell recruitment to the peritoneal cavity following OrV via the CXCR3 and its ligands. To test this, mice were depleted of NK cells and treated with either OrV or PBS. After 5 days, more CD8<sup>+</sup> T cells were



recovered from the peritoneal cavity of mice treated with OrfV when the NK compartment was intact (figure 6B), and these CD8<sup>+</sup> T cells also expressed higher levels of CXCR3 (figure 6C,D). This trend was lost when NK cells were depleted. To translate this to human ovarian cancer, the ICGC ovarian cancer dataset was interrogated for the expression of CXCR3 and its ligands. Using the gene signature for NK cells, we binned patient samples into NK high (highest third of NK signature expression) and NK low (lowest third). Patients with high NK-cell signatures expressed more CXCR3 ligands (figure 6E). Along similar lines, patients with high CD8<sup>+</sup> T-cell signatures had higher expression of CXCL9, CXCL10, and CXCL11 (figure 6F). In concordance with our observations in the mouse, patient samples with high CD8<sup>+</sup> T cells had higher expression of CXCR3, suggesting that NK cells may be attracting T cells to the TME in human ovarian cancer through CXCR3 signaling (figure 6G).

### **OrfV therapy does not synergize with immune checkpoint blockade but can be combined with surgical removal of the primary tumor-bearing ovary for optimal outcome**

ICB, including targeting the PD-1 axis, has shown considerable success in the clinic for treating multiple types of cancer. Blocking the interaction of PD-1 with its ligands PD-L1 and PD-L2 reverses the suppression of T cells and NK cells.<sup>14 15</sup> Recently, VACV was successfully combined with anti-PD-L1 in colon and ovarian cancer models.<sup>21</sup> Targeting PD-1 instead of its ligand has also been tested with VACV, with favorable results against murine fibrosarcoma.<sup>43</sup> We hypothesized that combining OrfV therapy for advanced-stage ovarian cancer with anti-PD-1 would improve the function of antitumor NK cells and CTLs. ID8 cells treated with OrfV upregulated PD-L1 within 6 hours, but cells infected with VACV did not (figure 7A,B). To investigate anti-PD-1 intervention, ID8 tumor-bearing mice (n=8) were treated with three doses of OrfV or VACV and then six doses of checkpoint blockade (figure 7C). Anti-PD-1 therapy alone was effective against ID8 tumor progression, as were OrfV and VACV monotherapies (figure 7D,E). However, the combination of either virus with checkpoint blockade did not extend survival in our murine model of advanced EOC. This suggests that PD-1-driven suppression of T cells and/or NK cells does not negatively impact OrfV-mediated therapy.

Cytoreduction surgery followed by chemotherapy is a common treatment for advanced EOC. Surgery is immune suppressive and has been linked to enhanced risk of metastasis.<sup>44</sup> Others have shown that intervention with OVs, including OrfV, during the suppressive perioperative window can reduce the risk of metastasis, primarily by improving NK-cell function.<sup>23 45</sup> We hypothesized that OrfV would be effective in combination with cytoreduction surgery to eliminate residual disease. To test this, mice (n=8) were implanted with ID8 tumor cells in the left ovarian bursa, which was surgically removed 60 days later. Resected ovaries were confirmed to have tumors in the ovarian bursa by histology (figure 7F). Mice recovered

from surgery for 48 hours before being treated with standard OrfV therapy. Primary tumor removal alone did not significantly enhance survival compared with controls (figure 7G). However, mice that had primary tumor removal surgery followed by OrfV therapy survived longer than mice that only received OrfV, with a median survival of 132 days. At the end of the experiment, 205 days post-tumor challenge, one mouse receiving the combination of primary tumor removal and OrfV therapy had no sign of ascites or secondary lesions, indicating OrfV as particularly effective when used to combat immune suppression following surgery.

## **DISCUSSION**

This study demonstrates that OrfV, especially in combination with cytoreduction surgery, is a promising antigen-agnostic immunotherapy platform for ovarian cancer. OrfV is valuable for its ability to directly kill tumor cells and to initiate a complex antitumor immune response involving multiple anticancer effector mechanisms. The bulk of the antitumor mechanism is mediated by NK cells and is supported by cDC1s, T cells and tumor-directed antibodies. This is of particular interest, given the recently unveiled importance of NK:cDC1 interactions controlling tumor progression in numerous cancer types.<sup>20</sup>

OrfV was effective at killing murine and human ovarian cancer cells lines in vitro, despite exhibiting limited production of new virus particles within these cells. While our data indicate that OrfV replication is limited in the human ovarian cancer lines investigated, OrfV has been shown to infect and replicate in other human cancer cell lines of the NCI-60 panel.<sup>22</sup> Future studies examining OrfV oncolysis and replication in a larger panel of patient-derived ovarian cancer samples are warranted to elucidate the clinical potential of OrfV against human ovarian cancers.

A single dose of OrfV delivered either intravenously or intraperitoneally was effective at reducing ascites fluid acutely following virus administration. Tumor cell lines derived from the ascites fluid of untreated animals were exquisitely sensitive to OrfV oncolysis when compared with parental ID8 cells. A prolonged reduction in ascites was observed following a single dose of OrfV, but there was no reduction of primary tumors in treated animals. Additionally, OrfV treatment reduced the formation of secondary lesions. This highlights that OrfV may be particularly effective at clearing residual disease when used in combination with surgical removal of the primary tumor, as shown in our studies.

The potential of OVs to elicit antitumor antibody responses has been understudied, apart from the impact of virus-neutralizing antibodies on the systemic delivery of OVs. ID8 tumor-directed antibodies were detected following OrfV intervention and the magnitude of the tumor-directed antibody correlated with enhanced survival. A major mechanism of NK activation and target-cell killing is through antibody-dependent cytotoxicity

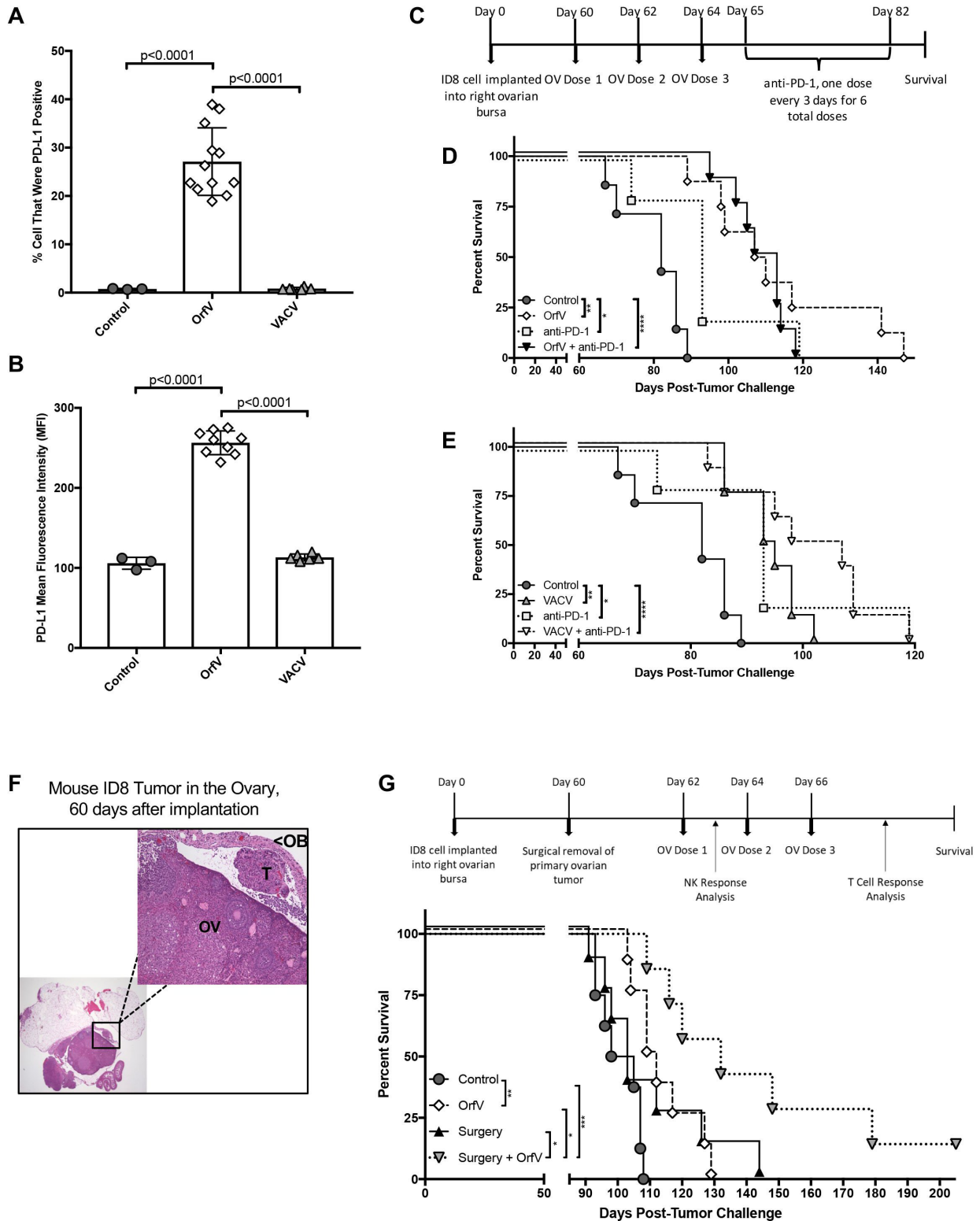


**Figure 7** OrV therapy is not improved by immune checkpoint blockade but combines with primary tumor resection. (A) Percent ID8 cells positive for PD-L1 expression following OrV or VACV infection as determined by flow cytometry. (B) The mean fluorescent intensity of PD-L1 from ID8 cells following OrV or VACV infection as determined by flow cytometry. (C) Treatment schematic testing the in vivo combination therapy of OrV or VACV with anti-PD-1. (D) Log-rank analysis of ID8 tumor-bearing mice treated with OrV alone or in combination with anti-PD-1 following the treatment schema in C. (E) Log-rank analysis of ID8 tumor-bearing mice treated with VACV alone or in combination with anti-PD-1 following the treatment schema in C. (F) Representative histological section of an ID8 tumor-bearing ovary surgically removed 60 days following tumor implantation. (G) ID8 mice underwent tumor-bearing ovary resection surgery 60 days following tumor implantation and were then treated with OrV as per the schematic (top). Survival comparisons were conducted by log-rank test. \* $P < 0.05$ , \*\* $P < 0.01$ , \*\*\* $P < 0.001$ , \*\*\*\* $p < 0.0001$ . OB, ovarian bursa; OrV, Orf virus; OV, ovary; T, tumor; VACV, vaccinia virus.

(ADCC), wherein target cells labeled by antibody are recognized by Fc receptors on NK cells.<sup>46</sup> An advantage of boosting tumor-directed antibodies using antigen-agnostic strategies includes generating antibodies against multiple tumor targets. This theoretically improves the likelihood of producing functional tumor-directed antibodies and reduces the risk of tumor escape by antigen loss. However, the potential for autoreactive antibody production requires assessment. Tumor-directed humoral responses may sustain effector NK-cell function beyond the primary NK-cell response through ADCC activation of NK cells and the subsequent production of IFN- $\gamma$  and TNF- $\alpha$ .<sup>47</sup> Future studies should aim to elucidate the contribution of ADCC by NK cells to therapeutic outcome and include functional experiments to definitively assess the importance of tumor-directed antibodies.

This study underscores the potency of OrfV as an anti-tumor NK-cell stimulant. Transcriptomic analysis of NK cells enriched from the ascites of OrfV-treated animals clearly demonstrate that OrfV triggers an inflammatory response from NK cells that includes expression of inflammatory cytokines, cytotoxic effectors, and genes involved in metabolism and cell division. The complexity of the data provides numerous avenues for exploring the antitumor effector phenotype of NK cells in more detail. NK-cell subsets are remarkably diverse and are now thought to participate in effector, regulatory, and memory functions.<sup>48</sup> Our study focused on a classical definition of NK cells, but future studies are under way to build on the transcriptomics data presented here to better define the NK subsets that respond to OrfV. NK cells may kill OrfV-infected tumor cells through virus-mediated downregulation of MHC class I,<sup>49</sup> which could limit virus spread. However, direct infection of tumor cells may not be required for NK-mediated killing, and the efficacy of replication-defective OrfV was not tested. An important question to be addressed is whether NK cells themselves are targets for OrfV infection and if replication-defective OrfV can activate the same gene expression profile in NK cells as replicating virus.

In response to OrfV, NK cells produced IFN- $\gamma$  and induced inflammatory cDC1s to produce IL-12, a critical cytokine for NK cells.<sup>50</sup> OrfV-treated animals lacking NK cells were unable to mount tumor-specific CD8<sup>+</sup> T-cell responses. This may be due to insufficient cDC1 antigen presentation and costimulation. Optimal NK help for cDC1s requires type I IFN production and intact IFN signaling in DCs.<sup>16</sup> We observed that supernatant from OrfV-infected ID8 cells induced DC production of IL-12, which could be driven by IFN. Genetic ablation of cDC1s attenuated both NK and tumor-specific CTL responses, eliminating OrfV tumor control. This demonstrated that both NK and CTL responses depend on cDC1s. cDC1s may be an important target for enhancing OrfV therapy and OV therapies in general, given that most viruses induce interferon.

The codepletion of CD4<sup>+</sup> and CD8<sup>+</sup> T cells using anti-Thy1.2 did not affect survival outcome. Despite this,

ID8-specific T cells were detected in the circulation of OrfV-treated animals, and CD8<sup>+</sup> T cells were recruited to the peritoneal cavity along a CXCR3: CXCL10 chemokine gradient. Additionally, OrfV rapidly upregulated PD-L1 on ID8 cells during infection. Anti-PD-1 therapy is particularly effective against tumors with a high neoantigen load,<sup>51</sup> and although OrfV monotherapy induced tumor-specific CTLs, they were dispensable for the primary response to therapy. A recent study with ID8 EOC highlighted the failure of neoantigen vaccines to induce T cell-mediated tumor control.<sup>52</sup> This was due to an impotent repertoire of functional antitumor CTL clones capable of recognizing tumor neoantigen. This may explain the lack of synergy with anti-PD-1 in our model and suggests that overcoming neoantigen insufficiencies by incorporating a tumor antigen into OrfV could dramatically improve T-cell responses and tumor control. Additionally, CTL targeting may be limited by low expression of MHC class I by ID8 cells, which we did not evaluate *in vivo*. Low MHC class I could also explain the relative potency of antigen-unrestricted NK cells. Intriguingly, NK cells play a role in anti-PD-1 ICB.<sup>14</sup> It is possible that we observed no clear benefit of anti-PD-1 because it was delivered 5 days after the first dose of virus, or near the end of the primary NK-cell response. Further studies are needed to characterize the role of the PD-1 axis in ovarian cancer in the context of NK and T-cell responses mediated by OrfV intervention. Additionally, the removal of NK cells by monoclonal antibody may have a compounding effect on tumor control as NK cells were a major source of CXCL10 in our experiments, and their removal may severely limit the recruitment of CXCR3<sup>+</sup> T cells to the TME.

Primary tumor removal surgery is a common treatment for advanced-stage ovarian cancer, but it is rarely curative. Surgery itself can increase the likelihood of metastatic disease through suppression of the immune system during the perioperative period.<sup>44</sup> OrfV intervention has been used to limit metastatic disease in preclinical models by preventing surgery-induced suppression of NK cells.<sup>23</sup> Shortly following surgery, NK cells are recruited but are weakly activated and produce low amounts of IFN. In a preclinical model using nephrectomy as the surgical insult, OrfV was delivered before B16F10 lung tumor challenge to prophylactically activate NK cells. Nephrectomies were conducted 1 hour following tumor challenge. In this setting, B16 tumor cell implantation in the lungs was dramatically reduced by oncolytic OrfV and its activation of NK cells.<sup>36</sup> Consistent with this, we observed a marked survival extension in mice undergoing surgery followed by OrfV when compared with virus or surgery alone. At the time of surgery, mice had a primary tumor and secondary lesions in the peritoneal cavity and ascites, representing a clinically relevant TME. We delayed OrfV intervention to 2 days following surgery, increasing the difficulty of treating secondary disease. Further experimentation is under way to determine the optimal timing for OrfV intervention in the perioperative window, as this could be particularly useful to translate to the clinic.



Of particular consideration when discussing the clinical potential of oncolytic OrfV is the chosen dose of virus. In this study, a dose of  $5 \times 10^7$  PFU was well tolerated when delivered to mice by intravenous or intraperitoneal administration. Doses as high as  $1 \times 10^9$  PFU have been administered without any notable adverse effects (data not shown). However, to clinically apply OrfV as a therapeutic agent against ovarian cancers will require additional dose optimization and safety studies within an acceptable larger rodent model and non-human primate. We recently optimized a method to generate large amounts of high quality, high titer, infectious OrfV<sup>24</sup> that could be scaled to support the translation of OrfV-derived technologies into the clinic.

In conclusion, OrfV is a multimechanistic antigen-agnostic immunotherapy effective against preclinical advanced-stage ovarian cancer. OrfV efficacy is tightly linked to NK cells that required cDC1 support. OrfV-activated NK cells were a major source of CXCL10 and stimulated recruitment of CD8<sup>+</sup> T cells to the ovarian TME. OrfV therapy also stimulated a robust tumor-directed antibody response, which may further support tumor control. Notably, these immunological effector pathways were also present in human ovarian cancer. There is a striking advantage to a therapeutic platform with such diversity when considering its application to the clinic. OrfV was especially effective when combined with primary tumor removal surgery, which is a common treatment modality. This highlights the potential for OrfV to be incorporated into the current treatment paradigm for ovarian cancer.

#### Author affiliations

- <sup>1</sup>Department of Pathobiology, University of Guelph, Guelph, Ontario, Canada  
<sup>2</sup>Department of Biomedical Sciences, University of Guelph, Guelph, Ontario, Canada  
<sup>3</sup>Molecular and Cellular Biology, University of Guelph, Guelph, Ontario, Canada  
<sup>4</sup>Department of Molecular and Cellular Biology, University of Guelph, Guelph, Ontario, Canada  
<sup>5</sup>Biodesign Institute, Arizona State University, Tempe, Arizona, USA

**Acknowledgements** We thank Campus Animal Facilities, University of Guelph, for animal care services.

**Contributors** JpVv, SKW, BWB, JJP, GM, and KK contributed to the conception and design of the research; JpVv, JJP, GM, BWB, and SKW contributed to the development of methodology; JpVv, SKW, BWB, KM, MAAM, JAM, LAS, MP, AAS, TMM, and EMK contributed to the acquisition of data; JpVv, SKW, BWB, MAAM, JC, JJP, GM, and KK contributed to the analysis and/or interpretation of data; JpVv, SKW, JAM, and BWB contributed to writing the manuscript; JpVv, SKW, JAM, BWB, MAAM, JC, JJP, GM, and KK contributed to reviewing and revising the manuscript. As the guarantor, SKW is responsible for the overall content.

**Funding** This research was supported by a New Investigator Award from the Terry Fox Research Institute to BWB (project number 1041) with partnering funds from The Smiling Blue Skies Cancer Fund and the Pet Trust Foundation. Basic science components of the research were supported by Discovery grants awarded to BWB and SKW by the Natural Sciences and Engineering Research Council of Canada (NSERC, grant numbers 436264 and 499834). Stipend funding was provided by Ontario Graduate Scholarship, Ontario Ministry of Agriculture and Rural Affairs Highly Qualified Personnel Scholarship and Ontario Veterinary College Graduate Scholarship (JpVv); Ontario Graduate Scholarship and Ontario Veterinary College Graduate Scholarship (JAM and LAS).

**Competing interests** None declared.

**Patient consent for publication** Not applicable.

**Ethics approval** The study was conducted according to the guidelines of the Declaration of Helsinki and approved by the Animal Care Committee of the University of Guelph (animal use protocol 3827, September 17, 2017) in accordance with Canadian Council on Animal Care guidelines.

**Provenance and peer review** Not commissioned; externally peer reviewed.

**Data availability statement** Data are available upon reasonable request.

**Supplemental material** This content has been supplied by the author(s). It has not been vetted by BMJ Publishing Group Limited (BMJ) and may not have been peer-reviewed. Any opinions or recommendations discussed are solely those of the author(s) and are not endorsed by BMJ. BMJ disclaims all liability and responsibility arising from any reliance placed on the content. Where the content includes any translated material, BMJ does not warrant the accuracy and reliability of the translations (including but not limited to local regulations, clinical guidelines, terminology, drug names and drug dosages), and is not responsible for any error and/or omissions arising from translation and adaptation or otherwise.

**Open access** This is an open access article distributed in accordance with the Creative Commons Attribution Non Commercial (CC BY-NC 4.0) license, which permits others to distribute, remix, adapt, build upon this work non-commercially, and license their derivative works on different terms, provided the original work is properly cited, appropriate credit is given, any changes made indicated, and the use is non-commercial. See <http://creativecommons.org/licenses/by-nc/4.0/>.

#### ORCID iD

Sarah K Wootton <http://orcid.org/0000-0002-5985-2406>

#### REFERENCES

- 1 Stewart C, Ralyea C, Lockwood S. Ovarian cancer: an integrated review. *Semin Oncol Nurs* 2019;35:151–6.
- 2 Evans DG, Gaarenstroom KN, Stirling D, *et al*. Screening for familial ovarian cancer: poor survival of BRCA1/2 related cancers. *J Med Genet* 2009;46:593–7.
- 3 Woodward ER, Sleightholme HV, Considine AM, *et al*. Annual surveillance by CA125 and transvaginal ultrasound for ovarian cancer in both high-risk and population risk women is ineffective. *BJOG* 2007;114:1500–9.
- 4 Ohman AW, Hasan N, Dinulescu DM. Advances in tumor screening, imaging, and avatar technologies for high-grade serous ovarian cancer. *Front Oncol* 2014;4:322.
- 5 Goff BA. Advanced ovarian cancer: what should be the standard of care? *J Gynecol Oncol* 2013;24:83–91.
- 6 Oronsky B, Ray CM, Spira AI, *et al*. A brief review of the management of platinum-resistant-platinum-refractory ovarian cancer. *Med Oncol* 2017;34:103.
- 7 Kipps E, Tan DSP, Kaye SB. Meeting the challenge of ascites in ovarian cancer: new avenues for therapy and research. *Nat Rev Cancer* 2013;13:273–82.
- 8 Russell SJ, Barber GN. Oncolytic viruses as antigen-agnostic cancer vaccines. *Cancer Cell* 2018;33:599–605.
- 9 Cook M, Chauhan A. Clinical application of oncolytic viruses: a systematic review. *Int J Mol Sci* 2020;21:ijms21207505. doi:10.3390/ijms21207505
- 10 Chaurasiya S, Chen NG, Fong Y. Oncolytic viruses and immunity. *Curr Opin Immunol* 2018;51:83–90.
- 11 Filley AC, Dey M. Immune system, friend or foe of oncolytic virotherapy? *Front Oncol* 2017;7:106.
- 12 Lanier JSMaLL. Natural killer cells in cancer immunotherapy. *An Rev Cancer Biol* 2019;3:77–103.
- 13 Hu W, Wang G, Huang D, *et al*. Cancer immunotherapy based on natural killer cells: current progress and new opportunities. *Front Immunol* 2019;10:1205.
- 14 Hsu J, Hodgins JJ, Marathe M, *et al*. Contribution of NK cells to immunotherapy mediated by PD-1/PD-L1 blockade. *J Clin Invest* 2018;128:4654–68.
- 15 Concha-Benavente F, Kansy B, Moskovitz J, *et al*. PD-L1 mediates dysfunction in activated PD-1<sup>+</sup> NK cells in head and neck cancer patients. *Cancer Immunol Res* 2018;6:1548–60.
- 16 Karimi K, Karimi Y, Chan J, *et al*. Type I IFN signaling on dendritic cells is required for NK cell-mediated anti-tumor immunity. *Innate Immun* 2015;21:626–34.
- 17 Mahmood S, Upreti D, Sow I, *et al*. Bidirectional interactions of NK cells and dendritic cells in immunotherapy: current and future perspective. *Immunotherapy* 2015;7:301–8.
- 18 Roberts EW, Broz ML, Binnewies M, *et al*. Critical role for CD103(+)CD141(+) dendritic cells bearing CCR7 for tumor antigen



- trafficking and priming of T cell immunity in melanoma. *Cancer Cell* 2016;30:324–36.
- 19 Barry KC, Hsu J, Broz ML, *et al.* A natural killer-dendritic cell axis defines checkpoint therapy-responsive tumor microenvironments. *Nat Med* 2018;24:1178–91.
  - 20 Böttcher JP, Bonavita E, Chakravarty P, *et al.* NK cells stimulate recruitment of cdc1 into the tumor microenvironment promoting cancer immune control. *Cell* 2018;172:e1014.
  - 21 Liu Z, Ravindranathan R, Kalinski P, *et al.* Rational combination of oncolytic vaccinia virus and PD-L1 blockade works synergistically to enhance therapeutic efficacy. *Nat Commun* 2017;8:14754.
  - 22 Rintoul JL, Lemay CG, Tai L-H, *et al.* ORFV: a novel oncolytic and immune stimulating parapoxvirus therapeutic. *Mol Ther* 2012;20:1148–57.
  - 23 Tai L-H, de Souza CT, Bélanger S, *et al.* Preventing postoperative metastatic disease by inhibiting surgery-induced dysfunction in natural killer cells. *Cancer Res* 2013;73:97–107.
  - 24 van Vloten JP, Minott JA, McAusland TM, *et al.* Production and purification of high-titer OrfV for preclinical studies in vaccinology and cancer therapy. *Mol Ther Methods Clin Dev* 2021;23:434–447.
  - 25 Karber G. Breitag Zur kollektiven behandlung pharmakologischer reihenver- suche. *Archiv fur Experimentelle Pathologie und Pharmakologie* 1931;162:480–3.
  - 26 Wulff NH, Tzatzaris M, Young PJ. Monte Carlo simulation of the Spearman-Kaerber TCID50. *J Clin Bioinforma* 2012;2:1–5.
  - 27 Bryan WR. Interpretation of host response in quantitative studies on animal viruses. *Ann N Y Acad Sci* 1957;69:698–728.
  - 28 Greenaway J, Henkin J, Lawler J, *et al.* ABT-510 induces tumor cell apoptosis and inhibits ovarian tumor growth in an orthotopic, syngeneic model of epithelial ovarian cancer. *Mol Cancer Ther* 2009;8:64–74.
  - 29 van Vloten JP, Santry LA, McAusland TM, *et al.* Quantifying antigen-specific T cell responses when using Antigen-Agnostic immunotherapies. *Mol Ther Methods Clin Dev* 2019;13:154–66.
  - 30 van Vloten JP, Klafuric EM, Karimi K, *et al.* Quantifying antibody responses induced by Antigen-Agnostic immunotherapies. *Mol Ther Methods Clin Dev* 2019;14:189–96.
  - 31 Dobin A, Davis CA, Schlesinger F, *et al.* STAR: ultrafast universal RNA-seq aligner. *Bioinformatics* 2013;29:15–21.
  - 32 Dillies M-A, Rau A, Aubert J, *et al.* A comprehensive evaluation of normalization methods for Illumina high-throughput RNA sequencing data analysis. *Brief Bioinform* 2013;14:671–83.
  - 33 Love MI, Huber W, Anders S. Moderated estimation of fold change and dispersion for RNA-seq data with DESeq2. *Genome Biol* 2014;15:1–21.
  - 34 Broz ML, Binnewies M, Boldajipour B, *et al.* Dissecting the tumor myeloid compartment reveals rare activating antigen-presenting cells critical for T cell immunity. *Cancer Cell* 2014;26:638–52.
  - 35 Russell S, Duquette M, Liu J, *et al.* Combined therapy with thrombospondin-1 type I repeats (3TSR) and chemotherapy induces regression and significantly improves survival in a preclinical model of advanced stage epithelial ovarian cancer. *Faseb J* 2015;29:576–88.
  - 36 Matuszewska K, Santry LA, van Vloten JP, *et al.* Combining vascular normalization with an oncolytic virus enhances immunotherapy in a preclinical model of advanced-stage ovarian cancer. *Clin Cancer Res* 2019;25:1624–38.
  - 37 Vile RG. The immune system in oncolytic immunovirotherapy: gospel, schism and heresy. *Mol Ther* 2018;26:942–6.
  - 38 Haeryfar SMM, Hoskin DW. Thy-1: more than a mouse pan-T cell marker. *J Immunol* 2004;173:3581–8.
  - 39 Hildner K, Edelson BT, Purtha WE, *et al.* Batf3 deficiency reveals a critical role for CD8alpha+ dendritic cells in cytotoxic T cell immunity. *Science* 2008;322:1097–100.
  - 40 McDonnell AM, Prosser AC, van Bruggen I, *et al.* CD8α+ DC are not the sole subset cross-presenting cell-associated tumor antigens from a solid tumor. *Eur J Immunol* 2010;40:1617–27.
  - 41 den Haan JM, Lehar SM, Bevan MJ. CD8(+) but not CD8(-) dendritic cells cross-prime cytotoxic T cells in vivo. *J Exp Med* 2000;192:1685–96.
  - 42 Mittal D, Vijayan D, Putz EM, *et al.* Interleukin-12 from CD103+ Batf3-dependent dendritic cells required for NK-cell suppression of metastasis. *Cancer Immunol Res* 2017;5:1098–108.
  - 43 Kleinpeter P, Fend L, Thiudellet C, *et al.* Vectorization in an oncolytic vaccinia virus of an antibody, a Fab and a scFv against programmed cell death -1 (PD-1) allows their intratumoral delivery and an improved tumor-growth inhibition. *Oncoimmunology* 2016;5:e1220467.
  - 44 Tohne S, Simmons RL, Tsung A. Surgery for cancer: a trigger for metastases. *Cancer Res* 2017;77:1548–52.
  - 45 Zhang J, Tai L-H, Ilkow CS, *et al.* Maraba MG1 virus enhances natural killer cell function via conventional dendritic cells to reduce postoperative metastatic disease. *Mol Ther* 2014;22:1320–32.
  - 46 Wang W, Erbe AK, Hank JA, *et al.* NK cell-mediated antibody-dependent cellular cytotoxicity in cancer immunotherapy. *Front Immunol* 2015;6:368.
  - 47 Simhadri VR, Dimitrova M, Mariano JL, *et al.* A human anti-M2 antibody mediates antibody-dependent cell-mediated cytotoxicity (ADCC) and cytokine secretion by resting and cytokine-preactivated natural killer (NK) cells. *PLoS One* 2015;10:e0124677.
  - 48 Nikzad R, Angelo LS, Aviles-Padilla K, *et al.* Human natural killer cells mediate adaptive immunity to viral antigens. *Sci Immunol* 2019;4:aat8116. doi:10.1126/sciimmunol.aat8116
  - 49 Rohde J, Emschermann F, Knittler MR, *et al.* Orf virus interferes with MHC class I surface expression by targeting vesicular transport and Golgi. *BMC Vet Res* 2012;8:114.
  - 50 Mailliard RB, Son Y-I, Redlinger R, *et al.* Dendritic cells mediate NK cell help for Th1 and CTL responses: two-signal requirement for the induction of NK cell helper function. *J Immunol* 2003;171:2366–73.
  - 51 McGranahan N, Furness AJS, Rosenthal R, *et al.* Clonal neoantigens elicit T cell immunoreactivity and sensitivity to immune checkpoint blockade. *Science* 2016;351:1463–9.
  - 52 Martin SD, Brown SD, Wick DA, *et al.* Low mutation burden in ovarian cancer may limit the utility of Neoantigen-Targeted vaccines. *PLoS One* 2016;11:e0155189.